Spring 1998

Fluid-structure interaction in Taylor-Couette flow

Martin Horst Willi Kempf
University of New Hampshire, Durham

FLUID-STRUCTURE INTERACTION IN TAYLOR-COUETTE FLOW

BY

Martin Horst Willi Kempf

B.S., University of Kassel, Germany (1988)
M.S., University of Kassel, Germany (1990)

DISSERTATION

Submitted to the University of New Hampshire
in Partial Fulfillment of
the Requirements for the Degree of

Doctor of Philosophy

in

Engineering

May 1998

This dissertation has been examined and approved.

Dissertation Director, John P. McHugh
Associate Professor of Mechanical Engineering

M. Robinson Swift
Professor of Mechanical Engineering

Dave W. Watt
Associate Professor of Mechanical Engineering

Kelly J. Black
Assistant Professor of Mathematics

Igor I. Tsukrov
Assistant Professor of Mechanical Engineering

04/30/98
Date

TABLE OF CONTENTS

DEDICATION

To W.K.

ACKNOWLEDGMENTS

My gratitude goes to my advisor Prof. John P. McHugh. without his support this dissertation would not have been possible.

I thank Prof. M. Robinson Swift. Prof. Dave W. Watt. Prof. Kelly J. Black and Prof. Igor I. Tsukrov for serving on my thesis committee.

Warm regards are sent to the secretaries Carol K. McCarthy and Tracey J. Harvey for their extensive help in administrative questions during my graduate studies at the University of New Hampshire.

Finally. I would like to mention the public bus system (COAST). and my Volkswagen Rabbit for providing a reliable local transportation in the rural seacoast area of New Hampshire.

BIOGRAPHY

Martin Horst Willi Kempf was born on the 27th of August 1965 in Saarbrücken, Germany. After finishing secondary school in Saarbrücken in 1983, he attended the University of Kassel, Germany, as a Mechanical Engineering major. There he obtained his Bachelor of Science in the fall of 1988. In 1989 and 1990 he performed his Master of Science thesis research at the German Aerospace Establishment, Göttingen, Germany. In the winter of 1990 he obtained his Master of Science in Mechanical Engineering from the University of Kassel. From the summer of 1991 to the summer of 1992 he took part in the post-graduate Diploma Course at the Von Karman Institute, Rhode Saint Genèse, Belgium. In the fall of 1992 he started graduate work in the PhD program of the Department of Mechanical Engineering at the University of New Hampshire, Durham, USA.

LIST OF SYMBOLS

$\mathbf{A}, \mathbf{B}$	matrices of generalized eigenproblem
A, B	constants of primary flow
$A_1^{(m)}, A_2^{(m)}, B_1^{(m)}, B_2^{(m)}$	coefficients of perturbation velocity $\tilde{u}_1$
B	body-force potential
b_m, b_n	coefficient in fourier-series
$\vec{b}$	eigenvector
$C1, C2, C3, C4$	coefficients of radial, and axial perturbation displacements
$D, D_r, D_{rr}, \nabla_r^2$	differential operators
$\vec{e}_r, \vec{e}_\theta, \vec{e}_z$	unit vectors in r, θ, z
$\vec{e}_R, \vec{e}_\Theta, \vec{e}_Z$	unit vectors in R, Θ, Z
$\vec{e}_x, \vec{e}_y, \vec{e}_z$	unit vectors in x, y, z
$\vec{e}_\alpha, \vec{e}_\beta, \vec{e}_\gamma$	unit vectors of α, β, γ
F	surface of fluid-elastic interface
$f, \overline{f}, f'$	arbitrary quantity, primary value of f, perturbation of f
G, H	implicit functions depending on F
g	function depending on Eulerian and Lagrangian coordinates
k	wave number
J	Jacobian
l_f	gap width
l_e	thickness of elastic layer
L	reference length
N	size of $N \times N$ matrix
$\vec{n}$	normal vector
$p, \overline{p}, p'$	pressure, primary pressure, perturbation pressure
$\vec{r}$	Eulerian coordinate vector
$\vec{R}$	Lagrangian coordinate vector
r, θ, z	cylindrical coordinates in Eulerian description
R, Θ, Z	cylindrical coordinates in Lagrangian description
R_0	radius of primary position of fluid-elastic interface
R_1	radius of inner cylinder
R_2	radius of fluid-elastic interface for stationary cylinders
R_3	radius of elastic-solid boundary at rigid base
Re	Reynolds number
$[S_{nm}]$	auxiliary matrix of $\mathbf{A}$, $\mathbf{B}$
t	time
T	Taylor number

$\vec{u}$	velocity vector
u, v, w	velocities in r, θ, z
$\overline{u}, \overline{v}, \overline{w}$	primary velocities in r, θ, z
u', v', w'	perturbation velocities in r, θ, z
u_1, v_1, w_1	perturbation velocities in r, θ, z as functions of r
$\bar{u}_1$	rescaled perturbation velocity u_1
u_R, u_Θ, u_Z	displacements in R, Θ, Z
$\overline{u}_R, \overline{u}_\Theta, \overline{u}_Z$	primary displacements in R, Θ, Z
u'_R, u'_Θ, u'_Z	perturbation displacements in R, Θ, Z
$u_{R_1}, u_{\Theta_1}, u_{Z_1}$	perturbation displacements in R, Θ, Z as functions of R
U	reference velocity
α, β, γ	radial, angular and axial deformations
α_n	parameter in Fourier-series expansion
δ	rescaled angular velocity ratio ξ
ϵ	small parameter
$\vec{\eta}$	displacement vector
μ, λ	Lamé parameters
ν	kinematic viscosity
ξ	angular velocity ratio $\frac{\Omega_0}{\Omega_1}$
ϕ	radius ratio $\frac{R_1}{R_0}$
ρ	density
σ^f_{ij}	stress component ij in fluid
σ^e_{ij}	stress component ij in elastic layer
χ	material constant as function of μ, λ
$\omega, \omega_r, \omega_i$	complex frequency, real part, imaginary part
Ω	angular velocity
Ω_0	angular velocity of outer cylinder
Ω_1	angular velocity of inner cylinder
ζ_r, ζ_R	rescaled radial coordinates of r, R
$\tilde{()}$	dimensionless value

LIST OF FIGURES

ABSTRACT

FLUID-STRUCTURE INTERACTION IN TAYLOR-COUETTE FLOW

by

Martin Horst Willi Kempf
University of New Hampshire, May, 1998

The linear stability of a viscous fluid between two concentric, rotating cylinders is considered. The inner cylinder is a rigid boundary and the outer cylinder has an elastic layer exposed to the fluid. The subject is motivated by flow between two adjoining rollers in a printing press. The governing equations of the fluid layer are the incompressible Navier-Stokes equations, and the governing equations of the elastic layer are Navier's equations. A narrow gap, neutral stability, and axisymmetric disturbances are assumed. The solution involves a novel technique for treating two layer stability problems, where an exact solution in the elastic layer is used to isolate the problem in the fluid layer. The results show that the presence of the elastic layer has only a slight effect on the critical Taylor numbers for the elastic parameters of modern printing presses. However, there are parameter values where the critical Taylor number is dramatically different than the classical Taylor-Couette problem.

CHAPTER 1

INTRODUCTION

The stability of a viscous fluid between two concentric, rotating cylinders is considered. The inner cylinder is a rigid boundary and the outer cylinder has a passive, homogeneous, elastic layer exposed to the fluid, see figure 1-1. The subject is motivated by flow in printing

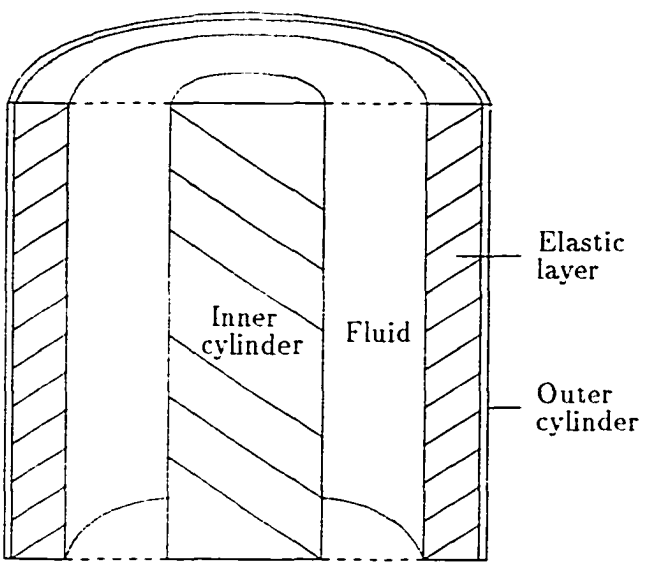

Figure 1-1: Schematic of the geometry.

presses, papermaking machines, and other industrial processes.

Schall & McHugh (1996) consider a similar problem with flow between an elastic layer and a rigid boundary for a printing press application. Water and ink are transported through

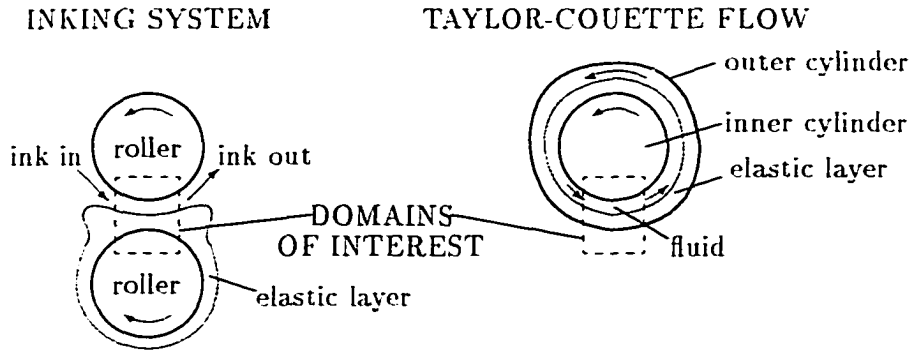

Figure 1-2: Schematic of two rollers in inking system compared with Taylor-Couette flow.

a high speed lithographic printing press by separate systems of parallel cylindrical rollers, cf. MacPhee (1979). The surfaces of adjoining rollers are always of different material. Some of the rollers are covered by an elastic material, similar to neoprene. The adjacent rollers are squeezed together, such that the elastic material is deformed to a concave shape, as shown in the schematic in figure 1-2. The dashed boxes in figure 1-2 indicate domains of the flow which is of interest. The flow between two adjoining rollers in a printing press is seen in figure 1-2 to be similar to Taylor-Couette flow with an elastic layer at the inner surface of the outer cylinder.

Flow between two rotating concentric rigid cylinders is classical Taylor-Couette flow, Taylor (1923), and is well known. The linear stability of Taylor-Couette flow is discussed in Chandrasekhar (1961) and Drazin & Reid (1981). Di Prima & Swinney (1985), Koschmieder (1993), and Chossat & Iooss (1994) provide comprehensive reviews of many aspects of the problem.

The stability of flow over compliant surfaces has been considered by a number of authors, mostly with regard to drag reduction. See for example Benjamin (1959, 1960, 1963), Duncan *et al.* (1985), Carpenter & Garrad (1986), Yeo (1987, 1988), Schall (1996), and Schall & McHugh (1996). Riley *et al.* (1988), and Carpenter (1990) provide reviews. It has

been found that the compliant coating can delay the classical instabilities due to the rigid boundary, such that transition to turbulent flow is postponed. Under certain circumstances the compliant coating can introduce new instabilities, so called surface modes, which can make the problem always unstable.

The stability of flow along a curved compliant wall is studied by Denier & Hall (1991). The results show that the presence of a compliant wall has a stabilizing effect to the Goertler vortices. However, this effect of the compliant wall is small, such that the stability of the flow is essentially the same as in the case of a rigid wall.

It is assumed here that the gap width between the cylinders is small in comparison to the radii of the cylinders. For classical Taylor-Couette flow with rigid cylinders Krueger *et al.* (1966) found that the critical disturbance is axisymmetric. In the case of rigid cylinders, Taylor (1923) concluded from his experiments that the onset of instability occurs as a secondary flow, and neutral stability can be assumed. Neutral stability, and axisymmetric disturbances are also assumed for the present case. For most parameter values, the results show either a relatively small stabilizing, or small destabilizing effect of the classical Taylor modes due to the elastic layer. However, a singularity of the critical Taylor mode is found, in the neighborhood of which the elastic layer has a large effect. No surface modes appeared in the stability analysis.

CHAPTER 2

GOVERNING EQUATIONS

2.1 Fluid Layer

The equation of motion for the fluid is the Navier-Stokes equation for incompressible flow, see for example Yih (1988). In cylindrical coordinates, and in dimensional form, these are

$$\frac{Du}{Dt} - \frac{v^2}{r} = -\frac{1}{\rho}\frac{\partial p}{\partial r} + \nu\left(\nabla^2 u - \frac{u}{r^2} - \frac{2}{r^2}\frac{\partial v}{\partial \theta}\right) - \frac{\partial \mathrm{B}}{\partial r}. \tag{2.1}$$

$$\frac{Dv}{Dt} + \frac{uv}{r} = -\frac{1}{\rho r}\frac{\partial p}{\partial \theta} + \nu\left(\nabla^2 v - \frac{v}{r^2} + \frac{2}{r^2}\frac{\partial u}{\partial \theta}\right) - \frac{1}{r}\frac{\partial \mathrm{B}}{\partial \theta}. \tag{2.2}$$

$$\frac{Dw}{Dt} = -\frac{1}{\rho}\frac{\partial p}{\partial z} + \nu\nabla^2 w - \frac{\partial \mathrm{B}}{\partial z}. \tag{2.3}$$

Equations (2.1), (2.2), (2.3), are the radial, azimuthal, and axial momentum equations, respectively. The radial coordinate is r, the azimuthal coordinate is θ, and the axial coordinate is z. The velocities u, v, w are in r, θ, z direction, respectively. The pressure is p, the density is ρ, the kinematic viscosity is ν, and the body force potential is B. The operators ∇^2, and $\frac{D}{Dt}$ are

$$\nabla^2 = \frac{\partial^2}{\partial r^2} + \frac{1}{r}\frac{\partial}{\partial r} + \frac{1}{r^2}\frac{\partial^2}{\partial \theta^2} + \frac{\partial^2}{\partial z^2}. \tag{2.4}$$

$$\frac{D}{Dt} = \frac{\partial}{\partial t} + u\frac{\partial}{\partial r} + \frac{v}{r}\frac{\partial}{\partial \theta} + w\frac{\partial}{\partial z}. \tag{2.5}$$

The continuity equation for incompressible flow in cylindrical coordinates, and in dimensional form is

$$\nabla \cdot \vec{u} = \frac{\partial u}{\partial r} + \frac{u}{r} + \frac{1}{r}\frac{\partial v}{\partial \theta} + \frac{\partial w}{\partial z} = 0, \tag{2.6}$$

where the velocity vector is

$$\vec{u} = u\vec{e}_r + v\vec{e}_\theta + w\vec{e}_z, \tag{2.7}$$

and $\vec{e}_r, \vec{e}_\theta, \vec{e}_z$ are unit vectors.

Introduce dimensionless radial, and axial coordinates

$$\hat{r} = \frac{r}{L}, \qquad \hat{z} = \frac{z}{L}, \tag{2.8}$$

respectively. The dimensionless velocities in r, θ, z direction are

$$\hat{u} = \frac{u}{U}, \qquad \hat{v} = \frac{v}{U}, \qquad \hat{w} = \frac{w}{U}, \tag{2.9}$$

respectively. The dimensionless time, and dimensionless pressure are

$$\hat{t} = t\frac{U}{L}, \qquad \hat{p} = \frac{p}{\rho U^2}, \tag{2.10}$$

respectively. The Reynolds Number is

$$\mathrm{Re} = \frac{LU}{\nu}. \tag{2.11}$$

The velocity U is a reference velocity, and L is a reference length. The reference quantities will be chosen later in the analysis.

After non-dimensionalising, equations (2.1) - (2.3) become

$$\frac{D\hat{u}}{D\hat{t}} - \frac{\hat{v}^2}{\hat{r}} = -\frac{\partial \hat{p}}{\partial \hat{r}} + \frac{1}{\mathrm{Re}}\left(\hat{\nabla}^2\hat{u} - \frac{\hat{u}}{\hat{r}^2} - \frac{2}{\hat{r}^2}\frac{\partial \hat{v}}{\partial \theta}\right). \tag{2.12}$$

$$\frac{D\hat{v}}{D\hat{t}} + \frac{\hat{u}\hat{v}}{\hat{r}} = -\frac{1}{\hat{r}}\frac{\partial \hat{p}}{\partial \theta} + \frac{1}{\mathrm{Re}}\left(\hat{\nabla}^2\hat{v} - \frac{\hat{v}}{\hat{r}^2} + \frac{2}{\hat{r}^2}\frac{\partial \hat{u}}{\partial \theta}\right). \tag{2.13}$$

$$\frac{D\hat{w}}{D\hat{t}} = -\frac{\partial \hat{p}}{\partial \hat{z}} + \frac{1}{\mathrm{Re}}\hat{\nabla}^2\hat{w}. \tag{2.14}$$

The continuity equation becomes

$$\hat{\nabla}\cdot\hat{\vec{u}} = \frac{\partial \hat{u}}{\partial \hat{r}} + \frac{\hat{u}}{\hat{r}} + \frac{1}{\hat{r}}\frac{\partial \hat{v}}{\partial \theta} + \frac{\partial \hat{w}}{\partial \hat{z}} = 0. \tag{2.15}$$

2.2 Elastic Layer

The equation of motion for a cylindrical elastic layer rotating with constant angular velocity is Navier's equation, see for example Love (1926), which is

$$(\lambda+\mu)\nabla(\nabla\cdot\vec{\eta}) + \mu\nabla^2\vec{\eta} + \rho\nabla \mathrm{B} = \rho\frac{\partial^2\vec{\eta}}{\partial t^2} - \rho\Omega^2 R\vec{e}_R. \tag{2.16}$$

The displacement vector is

$$\vec{\eta} = u_R\vec{e}_R + u_\Theta\vec{e}_\Theta + u_Z\vec{e}_Z. \tag{2.17}$$

where u_R, u_Θ, u_Z are displacements, and $\vec{e}_R, \vec{e}_\Theta, \vec{e}_Z$ are unit vectors. The operators ∇, $\nabla\cdot\vec{\eta}$, and ∇^2 are

$$\nabla = \vec{e}_R\frac{\partial}{\partial R} + \vec{e}_\Theta\frac{1}{R}\frac{\partial}{\partial \Theta} + \vec{e}_Z\frac{\partial}{\partial Z}, \tag{2.18}$$

$$\nabla\cdot\vec{\eta} = \frac{1}{R}\frac{\partial}{\partial R}(Ru_R) + \frac{1}{R}\frac{\partial u_\Theta}{\partial \Theta} + \frac{\partial u_Z}{\partial Z}. \tag{2.19}$$

$$\nabla^2 = \frac{1}{R}\frac{\partial}{\partial R}\left(R\frac{\partial}{\partial R}\right) + \frac{1}{R^2}\frac{\partial^2}{\partial \Theta^2} + \frac{\partial^2}{\partial Z^2}. \qquad (2.20)$$

The radial coordinate is R, the azimuthal coordinate is Θ, the axial coordinate is Z, the density is ρ, the Lamé parameters are λ and μ, the body force potential is B, and the angular velocity is Ω.

N.B., the Navier-Stokes equation employs an Eulerian coordinate system with the coordinates (r, θ, z), and Navier's equation employs a Lagrangian coordinate system with the coordinates (R, Θ, Z). Figure (2-1) illustrates the relation between the Eulerian and Lagrangian coordinate systems. The components of the Eulerian vector $\vec{r}$ are defined by r, θ, z.

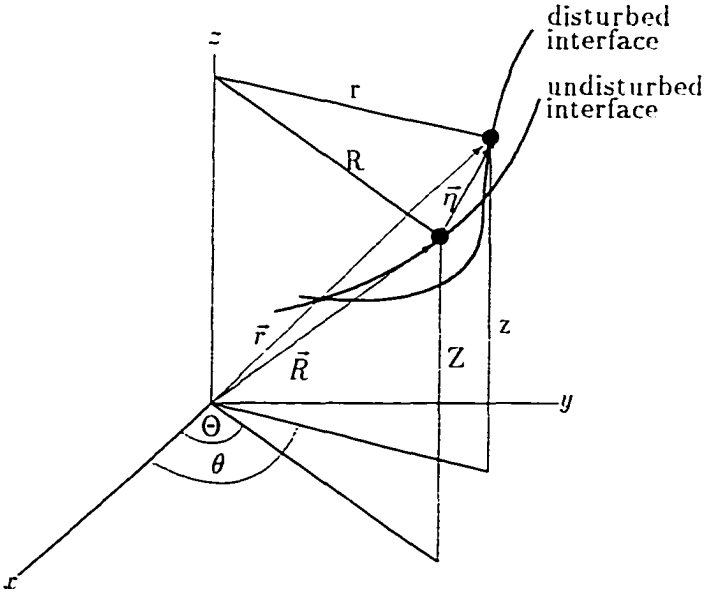

Figure 2-1: Eulerian and Lagrangian coordinate systems.

and the components of the Lagrangian vector $\vec{R}$ are defined by R, Θ, Z. The displacement vector $\vec{\eta}$ is the displacement of an interfacial particle from its initial position (undisturbed interface), to its displaced position (disturbed interface). Appendix A gives further details of the relation between $\vec{r}$ and $\vec{R}$.

Rescale as before, and obtain

$$\hat{R} = \frac{R}{L}, \qquad \hat{Z} = \frac{Z}{L}. \tag{2.21}$$

$$\hat{u}_R = \frac{u_R}{L}, \qquad \hat{u}_\Theta = \frac{u_\Theta}{L}, \qquad \hat{u}_Z = \frac{u_Z}{L}. \tag{2.22}$$

$$\hat{\lambda} = \frac{\lambda}{\rho L^2}, \qquad \hat{\mu} = \frac{\mu}{\rho L^2}. \tag{2.23}$$

The dimensionless time, $\hat{t}$, is given in equation (2.10). Navier's equations in cylindrical coordinates, without a body force, and in dimensionless form are

$$(\hat{\lambda}+\hat{\mu})\frac{\partial}{\partial \hat{R}}\left(\hat{\nabla}\cdot\hat{\vec{\eta}}\right) + \hat{\mu}\left(\hat{\nabla}^2\hat{u}_R - \frac{1}{\hat{R}^2}\left(\hat{u}_R + 2\frac{\partial \hat{u}_\Theta}{\partial \Theta}\right)\right) = \frac{\partial^2 \hat{u}_R}{\partial \hat{t}^2} - \Omega^2 R, \tag{2.24}$$

$$(\hat{\lambda}+\hat{\mu})\frac{1}{R}\frac{\partial}{\partial \Theta}\left(\hat{\nabla}\cdot\hat{\vec{\eta}}\right) + \hat{\mu}\left(\hat{\nabla}^2\hat{u}_\Theta - \frac{1}{\hat{R}^2}\left(\hat{u}_\Theta - 2\frac{\partial \hat{u}_R}{\partial \Theta}\right)\right) = \frac{\partial^2 \hat{u}_\Theta}{\partial \hat{t}^2}, \tag{2.25}$$

$$(\hat{\lambda}+\hat{\mu})\frac{\partial}{\partial \hat{Z}}\left(\hat{\nabla}\cdot\hat{\vec{\eta}}\right) + \hat{\mu}\hat{\nabla}^2\hat{u}_Z = \frac{\partial^2 \hat{u}_Z}{\partial \hat{t}^2}. \tag{2.26}$$

From here on, all quantities are dimensionless, and the circumflexes are dropped. If explicit distinction between dimensionless and dimensional quantities is necessary, only then dimensionless quantities are indicated by a circumflex.

CHAPTER 3

BOUNDARY CONDITIONS

There are three boundaries: the solid-fluid boundary between the rigid inner cylinder and the fluid, the fluid-elastic boundary between the fluid and the elastic layer, and the elastic-solid boundary between the elastic layer and the rigid base of the outer cylinder. A crossection

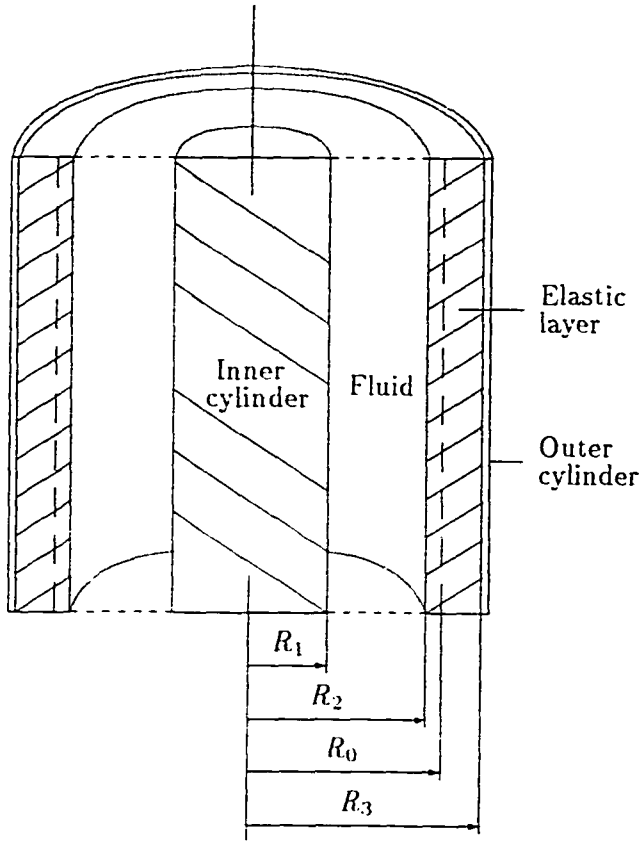

Figure 3-1: Crossection of the geometry.

of the geometry is shown in figure 3-1. The radius of the inner cylinder is R_1. The radius R_2 is the location of the interface between the fluid and elastic layer when the cylinders are stationary. The radius R_0 is the position of the same interface after the primary displacement has occurred. The elastic-solid boundary is at R_3. The following sections describe these boundary conditions in detail.

3.1 Interface between the Inner Cylinder and the Fluid Layer

At the solid-fluid interface between the rigid inner cylinder and the fluid, R_1, the velocity of the fluid perpendicular to the wall is

$$u = 0, \tag{3.1}$$

which is the "no-penetration condition". The velocity of the fluid in azimuthal direction is

$$v = \Omega_1 R_1, \tag{3.2}$$

which is equal to the speed of the wall, where Ω_1 is the angular velocity of the inner cylinder. The velocity of the fluid in z direction is

$$w = 0, \tag{3.3}$$

at R_1. The conditions (3.2), and (3.3) are the "no-slip conditions".

3.2 Interface between the Fluid Layer and the Elastic Layer

The deformation of the elastic layer, as a result of the interaction between the fluid and the elastic layer, requires special consideration. The description of the elastic layer in Lagrangian coordinates and the description of the fluid layer in Eulerian coordinates imposes a particular challenge on the derivation of the boundary conditions at this interface.

Two kinds of conditions have to be considered: the kinematic boundary condition and the dynamic boundary condition. The kinematic boundary condition says that fluid and elastic layer have the same velocity at the interface. The dynamic condition requires an equilibrium between the stress distributions of fluid and elastic layer on the interface.

3.2.1 Kinematic Boundary Conditions

The velocity field $\vec{u}(r, \theta, z)$ of the fluid at the interface between fluid layer and elastic layer has to be equal to the velocity of the elastic layer. Hence the kinematic condition is

$$\vec{u} = \frac{\partial \vec{\eta}}{\partial t}. \tag{3.4}$$

or

$$(u\vec{e}_r + v\vec{e}_\theta + w\vec{e}_z) = \left(\frac{\partial u_R}{\partial t}\vec{e}_R + \frac{\partial u_\Theta}{\partial t}\vec{e}_\Theta + \frac{\partial u_Z}{\partial t}\vec{e}_Z\right). \tag{3.5}$$

at this interface. Use equations in op. cit. appendix A, substitute equations (A.8), (A.9), and (A.10), into equation (3.5), which becomes

$$u\Big(\cos(\theta-\Theta)\vec{e}_R+\sin(\theta-\Theta)\vec{e}_\Theta\Big)+v\Big(-\sin(\theta-\Theta)\vec{e}_R+\cos(\theta-\Theta)\vec{e}_\Theta\Big)+w\vec{e}_Z$$
$$=\frac{\partial u_R}{\partial t}\vec{e}_R+\frac{\partial u_\Theta}{\partial t}\vec{e}_\Theta+\frac{\partial u_Z}{\partial t}\vec{e}_Z. \tag{3.6}$$

Collect terms of $\vec{e}_R$, $\vec{e}_\Theta$, and $\vec{e}_Z$.

$$\Big(u\cos(\theta-\Theta)-v\sin(\theta-\Theta)\Big)=\frac{\partial u_R}{\partial t}. \tag{3.7}$$

$$\Big(u\sin(\theta-\Theta)+v\cos(\theta-\Theta)\Big)=\frac{\partial u_\Theta}{\partial t}. \tag{3.8}$$

$$w=\frac{\partial u_Z}{\partial t}. \tag{3.9}$$

respectively. Equations (3.7), (3.8), and (3.9) are the kinematic boundary conditions at R_0 in radial, azimuthal, and axial direction, respectively.

3.2.2 Dynamic Boundary Conditions

The dynamic condition prescribes the equilibrium of the stress distributions of fluid and elastic layer on the interface. Small displacement theory is assumed for the elastic layer. Hence the stress components in the elastic layer depend only linearly on the strain components, and for this case, the stress tensor in the elastic layer is the same for a Lagrangian and Eulerian coordinate system. With this assumption of small displacements, the equilibrium between the stress tensor of the fluid, σ^f_{ij}, and the stress tensor of the elastic layer, σ^e_{ij}, on the interface is

$$\sigma^f_{ij}n_j=\sigma^e_{ij}n_j. \tag{3.10}$$

Appendix B gives a detailed derivation of the normal vector $\vec{n}$. The expanded form of the tensor equation (3.10) is

$$\sigma^f_{rr}n_r + \sigma^f_{r\theta}n_\theta + \sigma^f_{rz}n_z = \sigma^e_{RR}n_r + \sigma^e_{R\Theta}n_\theta + \sigma^e_{RZ}n_z, \tag{3.11}$$

$$\sigma^f_{\theta r}n_r + \sigma^f_{\theta\theta}n_\theta + \sigma^f_{\theta z}n_z = \sigma^e_{\Theta R}n_r + \sigma^e_{\Theta\Theta}n_\theta + \sigma^e_{\Theta Z}n_z, \tag{3.12}$$

$$\sigma^f_{zr}n_r + \sigma^f_{z\theta}n_\theta + \sigma^f_{zz}n_z = \sigma^e_{ZR}n_r + \sigma^e_{Z\Theta}n_\theta + \sigma^e_{ZZ}n_z. \tag{3.13}$$

The shear stresses for equilibrium conditions satisfy following identities, which are for the fluid

$$\sigma^f_{r\theta} = \sigma^f_{\theta r}, \qquad \sigma^f_{rz} = \sigma^f_{zr}, \qquad \sigma^f_{\theta z} = \sigma^f_{z\theta}, \tag{3.14}$$

and for the elastic layer they are

$$\sigma^e_{R\Theta} = \sigma^e_{\Theta R}, \qquad \sigma^e_{RZ} = \sigma^e_{ZR}, \qquad \sigma^e_{\Theta Z} = \sigma^e_{Z\Theta}. \tag{3.15}$$

The stress components in the fluid are

$$\sigma^f_{rr} = -p + \frac{2}{\mathrm{Re}}\frac{\partial u}{\partial r}, \tag{3.16}$$

$$\sigma^f_{\theta\theta} = -p + \frac{2}{\mathrm{Re}}\left(\frac{u}{r} + \frac{1}{r}\frac{\partial v}{\partial \theta}\right), \tag{3.17}$$

$$\sigma^f_{zz} = -p + \frac{2}{\mathrm{Re}}\frac{\partial w}{\partial z}, \tag{3.18}$$

$$\sigma^f_{r\theta} = \sigma^f_{\theta r} = \frac{1}{\mathrm{Re}}\left(\frac{\partial v}{\partial r} - \frac{v}{r} + \frac{1}{r}\frac{\partial u}{\partial \theta}\right), \tag{3.19}$$

$$\sigma^f_{rz} = \sigma^f_{zr} = \frac{1}{\mathrm{Re}}\left(\frac{\partial u}{\partial z} + \frac{\partial w}{\partial r}\right), \tag{3.20}$$

$$\sigma^f_{\theta z} = \sigma^f_{z\theta} = \frac{1}{\mathrm{Re}}\left(\frac{\partial v}{\partial z} + \frac{1}{r}\frac{\partial w}{\partial \theta}\right). \tag{3.21}$$

cf. Yih (1988). For small strain, the stress components in the elastic layer are

$$\sigma^{e}_{RR} = (\lambda + 2\mu)\frac{\partial u_R}{\partial R} + \lambda\left(\frac{u_R}{R} + \frac{\partial u_Z}{\partial Z} + \frac{1}{R}\frac{\partial u_\Theta}{\partial \Theta}\right). \tag{3.22}$$

$$\sigma^{e}_{\Theta\Theta} = (\lambda + 2\mu)\left(\frac{u_R}{R} + \frac{1}{R}\frac{\partial u_\Theta}{\partial \Theta}\right) + \lambda\left(\frac{\partial u_R}{\partial R} + \frac{\partial u_Z}{\partial Z}\right). \tag{3.23}$$

$$\sigma^{e}_{ZZ} = (\lambda + 2\mu)\frac{\partial u_Z}{\partial Z} + \lambda\left(\frac{\partial u_R}{\partial R} + \frac{u_R}{R} + \frac{1}{R}\frac{\partial u_\Theta}{\partial \Theta}\right). \tag{3.24}$$

$$\sigma^{e}_{R\Theta} = \sigma^{e}_{\Theta R} = \mu\left(\frac{\partial u_\Theta}{\partial R} - \frac{u_\Theta}{R} + \frac{1}{R}\frac{\partial u_R}{\partial \Theta}\right). \tag{3.25}$$

$$\sigma^{e}_{RZ} = \sigma^{e}_{ZR} = \mu\left(\frac{\partial u_Z}{\partial R} + \frac{\partial u_R}{\partial Z}\right). \tag{3.26}$$

$$\sigma^{e}_{\Theta Z} = \sigma^{e}_{Z\Theta} = \mu\left(\frac{\partial u_\Theta}{\partial Z} + \frac{1}{R}\frac{\partial u_Z}{\partial \Theta}\right). \tag{3.27}$$

cf. Love (1926).

3.3 Interface between the Elastic Layer and the Rigid Base

The elastic-solid interface at R_3 is the boundary between the elastic layer and the rigid base of the outer cylinder, cf. figure 3-1. The elastic layer is connected to the rigid base such that no slip occurs. Hence, the displacements at R_3 are

$$u_R = 0, \qquad u_\Theta = \Omega_0 R_3 t, \qquad u_Z = 0. \tag{3.28}$$

CHAPTER 4

PRIMARY SOLUTIONS

The variables of the fluid and the elastic layer are decomposed into a primary value and a perturbation part, e.g. the arbitrary physical quantity

$$f = \overline{f} + f'. \tag{4.1}$$

where $\overline{f}$ is the primary value of f, and f' is the perturbation of f. This procedure is known as the "Reynolds decomposition", see for example Yih (1988). The present chapter describes the primary flow, the primary displacements, and the boundary conditions of the primary values.

4.1 Primary Flow

Taylor-Couette flow is parallel shear flow between two concentric cylinders. It is well known, see for example Taylor (1923) or Chandrasekhar (1961). The primary velocity for axisymmetric, steady motion between infinite long cylinders in the r, θ, z directions is

$$\overline{u} = 0, \tag{4.2}$$

$$\overline{v} = Ar + \frac{B}{r}, \tag{4.3}$$

$$\overline{w} = 0. \tag{4.4}$$

respectively. The primary pressure is

$$\overline{p} = \frac{A^2}{2} r^2 + 2AB \ln(r) - \frac{B^2}{2} \frac{1}{r}. \tag{4.5}$$

The constants A and B are

$$A = \frac{\Omega_1 R_1^2 - \Omega_0 R_0^2}{R_1^2 - R_0^2} = \Omega_1 \frac{\varphi^2 - \xi}{\varphi^2 - 1}, \tag{4.6}$$

$$B = \frac{R_1^2 R_0^2 (\Omega_0 - \Omega_1)}{R_1^2 - R_0^2} = R_1^2 \Omega_1 \frac{\xi - 1}{\varphi^2 - 1}. \tag{4.7}$$

where the radius ratio, and the angular velocity ratio are

$$\varphi = \frac{R_1}{R_0}. \tag{4.8}$$

$$\xi = \frac{\Omega_0}{\Omega_1}. \tag{4.9}$$

respectively. The angular velocity of the outer cylinder is Ω_0. As previously mentioned, Ω_1 is the angular velocity of the inner cylinder. The radii of the primary position of the fluid-elastic interface, and of the inner cylinder are R_0, and R_1, respectively, cf. figure 3-1.

4.2 Primary Displacement

For steady rotation, and axisymmetric conditions around the z axis the primary displacements, $\overline{u}_R$ and $\overline{u}_\Theta$, depend on R.

Solving the differential equations (2.24), the primary displacement in radial direction is

$$\overline{u}_R = \frac{\overline{p}(R_0)}{2R}\frac{R_3^2 - R^2}{\lambda + \mu\left(1 + \left(\frac{R_3}{R_0}\right)^2\right)} + \\ + \frac{\Omega_0}{8(\lambda + 2\mu)}\frac{1}{R}\left(R_3^4 - R^4 - R_0^2(R_3^2 - R^2)\frac{2\lambda + \mu\left(3 + \left(\frac{R_3}{R_0}\right)^4\right)}{\lambda + \mu\left(1 + \left(\frac{R_3}{R_0}\right)^2\right)}\right). \quad (4.10)$$

N.B. that $\overline{u}_R$ depends on the primary pressure in the fluid at the interface.

$$\overline{p}(R_0) = \frac{A^2}{2}R_0^2 + 2AB\ln(R_0) - \frac{B^2}{2}\frac{1}{R_0^2}. \quad (4.11)$$

Solving equation (2.25), the primary displacement in azimuthal direction is

$$\overline{u}_\Theta = \frac{B}{\mu \mathrm{Re}}\left(\frac{1}{R} - \frac{R}{R_3^2}\right) + \Omega_0 R t. \quad (4.12)$$

The term $\Omega_0 R t$ in equation (4.12) is a function of time, and appears due to the linear increase of the primary displacement $\overline{u}_\Theta$ with respect to the stationary reference system. The primary displacement in the Z-direction is zero.

4.3 Boundary Conditions

The primary velocity at R_1 is

$$\overline{u} = 0. \qquad \overline{v} = \Omega_1 R_1. \qquad \overline{w} = 0. \quad (4.13)$$

The primary velocity at R_0 is

$$\overline{u} = 0. \qquad \overline{v} = \Omega_0 R_0, \qquad \overline{w} = 0. \tag{4.14}$$

The primary displacement at R_0 is

$$\begin{aligned} \overline{u}_R &= \frac{\overline{p}(R_0)}{2R_0} \frac{R_3^2 - R_0^2}{\lambda + \mu\left(1 + \left(\frac{R_1}{R_0}\right)^2\right)} + \\ &+ \frac{\Omega_0}{8(\lambda + 2\mu)} \frac{1}{R_0} \left(R_3^4 - R_0^4 - R_0^2(R_3^2 - R_0^2) \frac{2\lambda + \mu\left(3 + \left(\frac{R_1}{R_0}\right)^4\right)}{\lambda + \mu\left(1 + \left(\frac{R_1}{R_0}\right)^2\right)} \right). \end{aligned} \tag{4.15}$$

$$\overline{u}_\Theta = \frac{B}{\mu \mathrm{Re}} \left(\frac{1}{R_0} - \frac{R_0}{R_3^2} \right) + \Omega_0 R_0 t. \tag{4.16}$$

The primary velocity of the elastic layer in azimuthal direction is

$$\frac{\partial \overline{u}_\Theta}{\partial t} = \Omega_0 R_0, \tag{4.17}$$

which is the primary velocity of the fluid at R_0, cf. equation (4.14).

The primary displacement at R_3 is

$$\overline{u}_R = 0. \qquad \overline{u}_\Theta = \Omega_0 R_3 t. \qquad \overline{u}_Z = 0. \tag{4.18}$$

CHAPTER 5

EQUATIONS GOVERNING THE PERTURBATION

The perturbation equations for the fluid layer and the elastic layer are determined by separating the physical quantities into primary and disturbance parts, linearizing the equations, and subtracting primary solutions.

5.1 Fluid Layer

The Navier-Stokes equations, (2.12) - (2.14), after linearizing about the primary flow, are

$$\frac{\partial u'}{\partial t} + \frac{\overline{V}}{r}\frac{\partial u'}{\partial \theta} - 2\left(A + \frac{B}{r^2}\right)v' = -\frac{\partial p'}{\partial r} + \frac{1}{\mathrm{Re}}\left(\frac{\partial}{\partial r}\left(\frac{1}{r}\frac{\partial (ru')}{\partial r}\right) + \frac{1}{r^2}\frac{\partial^2 u'}{\partial \theta^2} + \frac{\partial^2 u'}{\partial z^2} - \frac{2}{r^2}\frac{\partial v'}{\partial \theta}\right). \tag{5.1}$$

$$\frac{\partial v'}{\partial t} + \frac{\overline{V}}{r}\frac{\partial v'}{\partial \theta} + 2Au' = -\frac{1}{r}\frac{\partial p'}{\partial \theta} + \frac{1}{\mathrm{Re}}\left(\frac{\partial}{\partial r}\left(\frac{1}{r}\frac{\partial (rv')}{\partial r}\right) + \frac{1}{r^2}\frac{\partial^2 v'}{\partial \theta^2} + \frac{\partial^2 v'}{\partial z^2} + \frac{2}{r^2}\frac{\partial u'}{\partial \theta}\right). \tag{5.2}$$

$$\frac{\partial w'}{\partial t} + \frac{\overline{V}}{r}\frac{\partial w'}{\partial \theta} = -\frac{\partial p'}{\partial z} + \frac{1}{\mathrm{Re}}\left(\frac{1}{r}\frac{\partial}{\partial r}\left(r\frac{\partial w'}{\partial r}\right) + \frac{1}{r^2}\frac{\partial^2 w'}{\partial \theta^2} + \frac{\partial^2 w'}{\partial z^2}\right). \tag{5.3}$$

where the primes denote a perturbation quantity. Similarly, the continuity equation, (2.15), becomes

$$\frac{u'}{r} + \frac{\partial u'}{\partial r} + \frac{1}{r}\frac{\partial v'}{\partial \theta} + \frac{\partial w'}{\partial z} = 0. \tag{5.4}$$

The equations are now reduced. Eliminate the pressure between equations (5.1), and (5.3), by cross differentiation to obtain

$$
\begin{aligned}
&-\frac{\partial^2 u'}{\partial t \partial z} - \frac{\partial}{\partial z}\left(\frac{\overline{V}}{r}\frac{\partial u'}{\partial \theta}\right) + 2\left(A + \frac{B}{r^2}\right)\frac{\partial v'}{\partial z} + \\
&+\frac{1}{\mathrm{Re}}\frac{\partial}{\partial z}\left(\frac{\partial}{\partial r}\left(\frac{1}{r}\frac{\partial (ru')}{\partial r}\right) + \frac{1}{r^2}\frac{\partial^2 u'}{\partial \theta^2} + \frac{\partial^2 u'}{\partial z^2} - \frac{2}{r^2}\frac{\partial v'}{\partial \theta}\right) \\
= \; &-\frac{\partial^2 w'}{\partial t \partial r} - \frac{\partial}{\partial r}\left(\frac{\overline{V}}{r}\frac{\partial w'}{\partial \theta}\right) + \frac{1}{\mathrm{Re}}\frac{\partial}{\partial r}\left(\frac{1}{r}\frac{\partial}{\partial r}\left(r\frac{\partial w'}{\partial r}\right) + \frac{1}{r^2}\frac{\partial^2 w'}{\partial \theta^2} + \frac{\partial^2 w'}{\partial z^2}\right). \qquad (5.5)
\end{aligned}
$$

Ali & Herron (1996) have shown, that Taylor-Couette flow with rigid walls is linearly stable with respect to two-dimensional disturbances lying in a plane perpendicular to the axis of the cylinders. Krueger *et al.* (1966) found a critical value of $\xi = -0.78$ for the classical Taylor-Couette flow, above which the critical disturbance is axisymmetric and below which it is non-axisymmetric. In the elastic layer case axisymmetric disturbances are assumed, and the variables are separated using

$$u' = u_1(r)\cos(kz)e^{\omega t}. \qquad (5.6)$$

$$v' = v_1(r)\cos(kz)e^{\omega t}. \qquad (5.7)$$

$$w' = w_1(r)\sin(kz)e^{\omega t}. \qquad (5.8)$$

These normal-mode solutions of the perturbation velocities u', v', w' are composed of amplification terms, represented by the coefficients, $u_1(r)$, $v_1(r)$, $w_1(r)$, which are functions of r, and the spatial, and temporal propagation terms, represented by the trigonometric, and exponential terms, respectively. The wave number is k, and the frequency is ω. Substitute

equations (5.6) - (5.8) into equations (5.5), (5.2), and (5.4), which become

$$-k\left(\nabla_*^2 - k^2 - \omega\mathrm{Re}\right)u_1 - 2\mathrm{Re}k\left(A + \frac{B}{r^2}\right)v_1 = \left(\nabla_*^2 - k^2 - \omega\mathrm{Re}\right)\frac{dw_1}{dr}, \tag{5.9}$$

$$\left(\nabla_*^2 - k^2 - \omega\mathrm{Re}\right)v_1 = 2\mathrm{Re}Au_1. \tag{5.10}$$

$$\frac{u_1}{r} + \frac{du_1}{dr} + kw_1 = 0. \tag{5.11}$$

The operator ∇_*^2 is

$$\nabla_*^2 = \frac{d^2}{dr^2} + \frac{1}{r}\frac{d}{dr} - \frac{1}{r^2}. \tag{5.12}$$

Introduce the differential operators

$$D = \frac{d}{dr}. \tag{5.13}$$

$$D_* = \frac{d}{dr} + \frac{1}{r}. \tag{5.14}$$

into equations (5.9) - (5.11), and note that

$$D_*D = \nabla_*^2 + \frac{1}{r^2} = \frac{d^2}{dr^2} + \frac{1}{r}\frac{d}{dr}. \tag{5.15}$$

$$D_{**} = DD_* = \nabla_*^2 = \frac{d^2}{dr^2} + \frac{1}{r}\frac{d}{dr} - \frac{1}{r^2}. \tag{5.16}$$

Equations (5.9) - (5.11) become

$$-k\left(DD_* - k^2 - \omega\mathrm{Re}\right)u_1 - 2\mathrm{Re}k\left(A + \frac{B}{r^2}\right)v_1 = \left(DD_* - k^2 - \omega\mathrm{Re}\right)Dw_1, \tag{5.17}$$

$$\left(DD_* - k^2 - \omega\mathrm{Re}\right)v_1 = 2\mathrm{Re}Au_1. \tag{5.18}$$

$$w_1 = -\frac{1}{k}D_*u_1. \tag{5.19}$$

Substitute equation (5.19) into equation (5.17), the following system of ordinary differential equations describing the disturbance of the fluid layer is obtained, cf. Chandrasekhar (1961).

$$(D_{**} - k^2 - \omega \mathrm{Re})(D_{**} - k^2)u_1 = 2k^2 \mathrm{Re}(A + \frac{B}{r^2})v_1, \tag{5.20}$$

$$(D_{**} - k^2 - \omega \mathrm{Re})v_1 = 2\mathrm{Re}Au_1. \tag{5.21}$$

5.2 Elastic Layer

The Navier equations, (2.24) - (2.26), after subtracting the primary displacement quantities, are

$$(\lambda + 2\mu)\left(\frac{\partial}{\partial R}\left(\frac{1}{R}\frac{\partial(Ru'_R)}{\partial R}\right) + \frac{\partial}{\partial \Theta}\frac{\partial}{\partial R}\left(\frac{u'_\Theta}{R}\right) + \frac{\partial^2 u'_Z}{\partial R \partial Z}\right) +$$
$$+\mu\left(\frac{1}{R^2}\frac{\partial^2 u'_R}{\partial \Theta^2} + \frac{\partial^2 u'_R}{\partial Z^2} - \frac{\partial}{\partial \Theta}\left(\frac{1}{R^2}\frac{\partial(Ru'_\Theta)}{\partial R}\right) - \frac{\partial^2 u'_Z}{\partial R \partial Z}\right) = \frac{\partial^2 u'_R}{\partial t^2}, \tag{5.22}$$

$$(\lambda + 2\mu)\left(\frac{\partial}{\partial \Theta}\left(\frac{1}{R^2}\frac{\partial(Ru'_R)}{\partial R}\right) + \frac{1}{R^2}\frac{\partial^2 u'_\Theta}{\partial \Theta^2} + \frac{1}{R}\frac{\partial^2 u'_Z}{\partial \Theta \partial Z}\right) +$$
$$+\mu\left(-\frac{\partial}{\partial \Theta}\frac{\partial}{\partial R}\left(\frac{u'_R}{R}\right) + \frac{\partial}{\partial R}\left(\frac{1}{R}\frac{\partial(Ru'_\Theta)}{\partial R}\right) + \frac{\partial^2 u'_\Theta}{\partial Z^2} - \frac{1}{R}\frac{\partial^2 u'_Z}{\partial \Theta \partial Z}\right) = \frac{\partial^2 u'_\Theta}{\partial t^2}, \tag{5.23}$$

$$(\lambda + 2\mu)\left(\frac{\partial}{\partial Z}\left(\frac{1}{R}\frac{\partial(Ru'_R)}{\partial R}\right) + \frac{1}{R}\frac{\partial^2 u'_\Theta}{\partial \Theta \partial Z} + \frac{\partial^2 u'_Z}{\partial Z^2}\right) +$$
$$+\mu\left(-\frac{\partial}{\partial Z}\left(\frac{1}{R}\frac{\partial(Ru'_R)}{\partial R}\right) - \frac{1}{R}\frac{\partial^2 u'_\Theta}{\partial \Theta \partial Z} + \frac{1}{R}\frac{\partial}{\partial R}\left(R\frac{\partial u'_Z}{\partial R}\right) + \frac{1}{R^2}\frac{\partial^2 u'_Z}{\partial \Theta^2}\right) = \frac{\partial^2 u'_Z}{\partial t^2}. \tag{5.24}$$

where u'_R, u'_Θ, u'_Z are the perturbation displacements. Reduce these equations by assuming axisymmetric disturbances and separate the variables using

$$u'_R = u_{R_1}(R)\cos(kZ)e^{\omega t}, \tag{5.25}$$

$$u'_\Theta = u_{\Theta_1}(R)\cos(kZ)e^{\omega t}, \tag{5.26}$$

$$u'_Z = u_{Z_1}(R)\sin(kZ)e^{\omega t}. \tag{5.27}$$

Substitute (5.25) - (5.27) into (5.22), (5.23), and (5.24),

$$\left((\lambda+2\mu)\nabla_*^2 - \mu k^2 - \omega^2)\right) u_{R_1} = -k(\lambda+\mu)\frac{du_{Z_1}}{dR}. \tag{5.28}$$

$$\left(\mu\nabla_*^2 - \mu k^2 - \omega^2\right) u_{\Theta_1} = 0, \tag{5.29}$$

$$\left(\mu\nabla_*^2 + \frac{\mu}{R} - (\lambda+2\mu)k^2 - \omega^2\right) u_{Z_1} = k(\lambda+\mu)\left(\frac{d}{dR} + \frac{1}{R}\right) u_{R_1}. \tag{5.30}$$

respectively. Using the previously defined differential operators, the final result is

$$\left(\chi D_{**} - k^2 - \frac{\omega^2}{\mu}\right) u_{R_1} = -k(\chi-1)Du_{Z_1}. \tag{5.31}$$

$$\left(D_{**} - k^2 - \frac{\omega^2}{\mu}\right) u_{\Theta_1} = 0, \tag{5.32}$$

$$\left(D_*D - \chi k^2 - \frac{\omega^2}{\mu}\right) u_{Z_1} = k(\chi-1)D_*u_{R_1}, \tag{5.33}$$

where

$$\chi = 2 + \frac{\lambda}{\mu}. \tag{5.34}$$

N.B. that the Lagrangian variable R is now used instead of the Eulerian variable r in the

above differential operators.

5.3 Boundary Conditions

5.3.1 Inner Cylinder - Fluid Layer Interface

The velocity at the rigid boundary R_1, equations (3.1) - (3.3), is perturbed, linearized, and the primary flow quantities subtracted, becomes

$$u' = 0. \qquad v' = 0. \qquad w' = 0. \tag{5.35}$$

Substitute equations (5.6) - (5.8), into equation (5.35), and obtain

$$u_1 = 0. \qquad v_1 = 0. \qquad w_1 = 0. \tag{5.36}$$

5.3.2 Fluid Layer - Elastic Layer Interface

The position of the perturbed elastic interface is unknown a priori. This problem is circumvented by expanding the kinematic and dynamic boundary conditions in a Taylor series about the primary displacement of the elastic layer, which is at (R_0, Θ_0, Z_0). Each term in these boundary conditions is expanded in the following manner

$$\begin{aligned} g\Big|_{\substack{R_0 + u'_R \\ \Theta_0 + \frac{u'_\Theta}{R_0} \\ Z_0 + u'_Z}} = {} & g\Big|_{\substack{R_0 \\ \Theta_0 \\ Z_0}} + \frac{\partial g}{\partial r}\Big|_{\substack{R_0 \\ \Theta_0 \\ Z_0}} u'_R + \frac{\partial g}{r\partial\theta}\Big|_{\substack{R_0 \\ \Theta_0 \\ Z_0}} u'_\Theta + \frac{\partial g}{\partial z}\Big|_{\substack{R_0 \\ \Theta_0 \\ Z_0}} u'_Z \\ & + \frac{\partial g}{\partial R}\Big|_{\substack{R_0 \\ \Theta_0 \\ Z_0}} u'_R + \frac{\partial g}{R\partial\Theta}\Big|_{\substack{R_0 \\ \Theta_0 \\ Z_0}} u'_\Theta + \frac{\partial g}{\partial Z}\Big|_{\substack{R_0 \\ \Theta_0 \\ Z_0}} u'_Z + O(\epsilon^2). \end{aligned} \tag{5.37}$$

where

$$g = g(r, \theta, z, R, \Theta, Z). \tag{5.38}$$

The parameter ϵ in equation (5.37) is small, but different from zero.

Perturb the kinematic conditions, (3.7) - (3.9), expand each term in the aforementioned Taylor series about R_0, linearize, and subtract the primary quantities. The kinematic conditions in the radial, azimuthal, and axial direction are

$$u' = \frac{\partial u'_R}{\partial t}, \tag{5.39}$$

$$v' + u'_R D\overline{v} = \frac{\partial u'_R}{\partial t}, \tag{5.40}$$

$$w' = \frac{\partial u'_Z}{\partial t}, \tag{5.41}$$

respectively, where the derivative of the primary flow at R_0 is

$$D\overline{v} = A - \frac{B}{R_0^2}. \tag{5.42}$$

The constants A, and B are given in equations (4.6), and (4.7). Substitute equations (5.6) - (5.8), and equations (5.25) - (5.27) into equations (5.39), (5.40), (5.41), and obtain

$$u_1 = \omega u_{R_1}, \tag{5.43}$$

$$v_1 + u_{R_1} D\overline{v} = \omega u_{\Theta_1} \tag{5.44}$$

$$-\frac{1}{k} D_* u_1 = \omega u_{Z_1}, \tag{5.45}$$

Equations (5.43) - (5.45) describe the disturbance of the kinematic boundary conditions.

Note, equation (5.19) has been substituted into equation (5.45).

The dynamic boundary conditions, equations (3.11) - (3.13), perturbed, expanded in a Taylor series about R_0, linearized, and the primary quantities subtracted, become

$$-p' + \frac{2}{\mathrm{Re}}\frac{\partial u'}{\partial r} = (\lambda + 2\mu)\frac{\partial u'_R}{\partial R} + \lambda\left(\frac{u'_R}{R_0} + \frac{\partial u'_Z}{\partial Z}\right). \tag{5.46}$$

$$\frac{1}{\mathrm{Re}}\left(\frac{\partial v'}{\partial r} - \frac{v'}{R_0}\right) = \mu\left(\frac{\partial u'_\Theta}{\partial R} - \frac{u'_\Theta}{R_0}\right). \tag{5.47}$$

$$\frac{1}{\mathrm{Re}}\left(\frac{\partial u'}{\partial z} + \frac{\partial w'}{\partial r}\right) = \mu\left(1 + 2\frac{d\overline{u}_R}{dR}\right)\frac{\partial u'_R}{\partial Z} + \mu\frac{\partial u'_Z}{\partial R}. \tag{5.48}$$

The derivative of the primary displacement in R direction at R_0 is

$$\begin{aligned}\frac{d\overline{u}_R}{dR} = & -\frac{\overline{p}(R_0)}{2R_0^2}\frac{R_0^2 + R_3^2}{\lambda + \mu\left(1 + \left(\frac{R_3}{R_0}\right)^2\right)} - \\ & -\frac{\Omega_0}{8(\lambda + 2\mu)}\frac{1}{R_0^2}\left(R_3^4 + 3R_0^4 - R_0^2(R_3^2 + R_0^2)\frac{2\lambda + \mu\left(3 + \left(\frac{R_3}{R_0}\right)^4\right)}{\lambda + \mu\left(1 + \left(\frac{R_3}{R_0}\right)^2\right)}\right).\end{aligned} \tag{5.49}$$

The primary pressure $\overline{p}(R_0)$ is given by equation (4.5). Assume an axisymmetric disturbance of the pressure using

$$p' = p_1(r)\cos(kz)e^{\omega t}. \tag{5.50}$$

Substitute equations (5.6) - (5.8), (5.25) - (5.27), and (5.50) into equations (5.46), (5.47), and (5.48), and obtain

$$-p_1 + \frac{2}{\mathrm{Re}}\frac{du_1}{dr} = (\lambda + 2\mu)\frac{du_{R_1}}{dR} + \lambda\left(\frac{u_{R_1}}{R_0} + ku_{Z_1}\right). \tag{5.51}$$

$$\frac{1}{\mathrm{Re}}\left(\frac{dv_1}{dr} - \frac{v_1}{R_0}\right) = \mu\left(\frac{du_{\Theta_1}}{dR} - \frac{u_{\Theta_1}}{R_0}\right). \tag{5.52}$$

$$\frac{1}{\mathrm{Re}}\left(-ku_1+\frac{dw_1}{dr}\right)=-\mu k\left(1+2\frac{d\overline{u}_R}{dR}\right)u_{R_1}+\mu\frac{du_{Z_1}}{dR}. \tag{5.53}$$

Substitute equations (5.8), and (5.50), into equation (5.3), and obtain

$$-p_1=\frac{1}{k\mathrm{Re}}\left(\nabla_*^2+\frac{1}{r^2}-k^2-\omega\mathrm{Re}\right)w_1. \tag{5.54}$$

Use the operators introduced in equations (5.13) - (5.16), and substitute equations (5.54), and (5.19) into equations (5.51), (5.52), and (5.53).

$$\left(-(D_*D-k^2-\omega\mathrm{Re})D_*+2k^2D\right)u_1=k^2\mathrm{Re}(\lambda+2\mu)Du_{R_1}+k^2\mathrm{Re}\lambda\left(\frac{u_{R_1}}{R_0}+ku_{Z_1}\right) \tag{5.55}$$

$$\left(D-\frac{1}{R_0}\right)v_1=\mu\mathrm{Re}\left(D-\frac{1}{R_0}\right)u_{\Theta_1}. \tag{5.56}$$

$$(k^2+D_{**})u_1=k^2\mathrm{Re}\mu(1+2D\overline{u}_R)u_{R_1}-k\mathrm{Re}\mu Du_{Z_1}. \tag{5.57}$$

respectively. Equations (5.55) - (5.57) describe the disturbance of the dynamic boundary conditions.

5.3.3 Elastic Layer - Rigid Base Interface

The zero-displacement conditions at R_3, equation (3.28), are perturbed, and become

$$u'_R=0. \qquad u'_\Theta=0. \qquad u'_Z=0. \tag{5.58}$$

Substitute equations (5.25) - (5.27) into equation (5.58), and obtain

$$u_{R_1}=0. \qquad u_{\Theta_1}=0. \qquad u_{Z_1}=0. \tag{5.59}$$

CHAPTER 6

NARROW GAP

The reference length is now chosen to be the fluid gap.

$$L = R_0 - R_1, \tag{6.1}$$

and the reference velocity is chosen to be the gap width times the angular velocity of the inner cylinder.

$$U = (R_0 - R_1)\,\Omega_1. \tag{6.2}$$

The Reynolds number becomes

$$\mathrm{Re} = \frac{(R_0 - R_1)^2\,\Omega_1}{\nu}. \tag{6.3}$$

Assume that the gap between the inner cylinder and the elastic layer is small, such that

$$R_0 - R_1 \ll \frac{1}{2}(R_1 + R_0). \tag{6.4}$$

Therefore, the dimensionless radii, defined in equations (2.8), and (2.21), are

$$r, R \gg 1. \tag{6.5}$$

The reciprocal of equation (6.5) is

$$\frac{1}{r} \cdot \frac{1}{R} - \epsilon. \tag{6.6}$$

Terms of order ϵ or higher are small and hence negligible in the narrow gap case. N.B. that there is no geometrical limitation imposed on the elastic layer. The differential operators (5.14) - (5.16) become

$$D_* - D. \tag{6.7}$$

$$D_* D - D^2. \tag{6.8}$$

$$D_{**} = D D_* - D^2. \tag{6.9}$$

In addition, the ranges of r and R are rescaled such that the new radial coordinates in the Eulerian, and Lagrangian coordinate systems are

$$\zeta_r = \frac{r - R_1}{l_f}, \tag{6.10}$$

$$\zeta_R = \frac{R - R_0}{l_e}. \tag{6.11}$$

respectively, and have domains from 0 to 1, as in Chandrasekhar (1961). The thickness of the fluid layer, which is the gap width, is

$$l_f = R_0 - R_1. \tag{6.12}$$

The gap width in the rescaled case becomes

$$l_f = 1. \tag{6.13}$$

The thickness of the elastic layer is

$$l_e = R_3 - R_0. \tag{6.14}$$

6.1 Fluid Layer

The disturbance equations for the fluid, (5.20), and (5.21), become

$$(D^2 - k^2 - \omega \mathrm{Re})(D^2 - k^2)\tilde{u}_1 = (1 + \delta\zeta_r)v_1. \tag{6.15}$$

$$(D^2 - k^2 - \omega \mathrm{Re})v_1 = -\mathrm{T}k^2\tilde{u}_1. \tag{6.16}$$

where

$$\delta = -(1 - \xi). \tag{6.17}$$

$$\mathrm{T} = -4\mathrm{Re}^2\frac{\phi^2 - \xi}{\phi^2 - 1}. \tag{6.18}$$

$$\tilde{u}_1 = \frac{1}{2k^2}\frac{1}{\mathrm{Re}}u_1. \tag{6.19}$$

$$D = \frac{d}{d\zeta_r}. \tag{6.20}$$

Note that T is the Taylor number.

6.2 Elastic Layer

The elastic layer equations (5.31) - (5.33) become

$$\left(D^2 - \frac{k^2 l_e^2}{\chi} - \frac{\omega^2 l_e^2}{\chi\mu}\right) u_{R_1} = k l_e \left(\frac{1}{\chi} - 1\right) D u_{Z_1}. \tag{6.21}$$

$$\left(D^2 - k^2 l_e^2 - \frac{\omega^2 l_e^2}{\mu}\right) u_{\Theta_1} = 0. \tag{6.22}$$

$$\left(D^2 - \lambda k^2 l_e^2 - \frac{\omega^2 l_e^2}{\mu}\right) u_{Z_1} = k l_e (\lambda - 1) D u_{R_1}. \tag{6.23}$$

where

$$D = \frac{d}{d\zeta_R}. \tag{6.24}$$

6.3 Kinematic Boundary Conditions

The kinematic boundary conditions (5.43) - (5.45) become

$$\tilde{u}_1 = \frac{1}{2k^2}\frac{1}{\mathrm{Re}}\omega u_{R_1}. \tag{6.25}$$

$$v_1 = \omega u_{\Theta_1} + R_1(1-\xi) u_{R_1}. \tag{6.26}$$

$$-D\tilde{u}_1 = \frac{1}{2k^2}\frac{1}{\mathrm{Re}}\omega u_{Z_1}. \tag{6.27}$$

where the term $R_1(1-\xi)$ in equation (6.26) has been rescaled with respect to the narrow gap.

6.4 Dynamic Boundary Conditions

The dynamic boundary conditions, (5.55) - (5.57), become

$$-2\left(D^2 - 3k^2 - \omega\mathrm{Re}\right) D\tilde{u}_1 = \frac{1}{l_e}(\lambda + 2\mu) D u_{R_1} + k\lambda u_{Z_1}. \tag{6.28}$$

$$D v_1 = \frac{\mu \mathrm{Re}}{l_e} D u_{\Theta_1}. \tag{6.29}$$

$$2(D^2+k^2)\tilde{u}_1 = \mu(1+2D\overline{u}_R)\,u_{R_1} - \frac{\mu}{kl_e}Du_{Z_1}. \tag{6.30}$$

Note, the differential operator D acting on a disturbance velocity is now defined by equation (6.20), and if acting on a disturbance displacement, D is defined by equation (6.24). The derivative of the primary radial displacement at R_0, equation (5.49), becomes

$$\begin{aligned} D\overline{u}_R \;=\; & -\frac{\overline{p}(R_0)}{2R_0^2}\frac{R_0^2+R_3^2}{\lambda+\mu\left(1+\left(\frac{R_3}{R_0}\right)^2\right)} - \\ & -\frac{\xi}{8(\lambda+2\mu)}\frac{1}{R_0^2}\left(R_3^4+3R_0^4-R_0^2(R_3^2+R_0^2)\frac{2\lambda+\mu\left(3+\left(\frac{R_3}{R_0}\right)^4\right)}{\lambda+\mu\left(1+\left(\frac{R_3}{R_0}\right)^2\right)}\right). \end{aligned} \tag{6.31}$$

where the primary pressure, equation (4.11), simplifies in the narrow gap case to

$$\overline{p}(R_0) = -\frac{1}{2}R_1^2\ln(R_0)\left(\frac{1}{2}R_1^2(1-\xi)-R_0^2(1-\xi)\xi\right) - \frac{1}{8}R_1R_0(3R_1-2R_0\xi). \tag{6.32}$$

From equations (6.12), and (6.13) the radii R_1, and R_0 have the relation

$$R_0 = R_1 + 1. \tag{6.33}$$

CHAPTER 7

SOLUTION OF PERTURBATION EQUATIONS

Taylor (1923) concluded from his experiments of Taylor-Couette flow between rigid cylinders that the principle of exchange of stabilities is valid. Davis (1969) and Yih (1972) verified Taylor's observations by mathematical proofs for certain speed ranges. For the present problem, it is also assumed that the principle of exchange of stabilities is valid. Hence, neutral stability is assumed and ω is set to zero.

The exchange of stabilities is explained with the schematics in figure 7-1, which show the temporal behavior of the disturbance solution. In general, instability may occur in fluid systems in an oscillating manner, as shown in the top two schematics in figure 7-1. For classical Taylor-Couette flow, however, instability occurs without oscillation ($\omega_i = 0$), as shown in the third schematic. Neutral stability means a parameter value which lies on the boundary between stability and instability, which means no growth or decay, and therefore $\omega_r = 0$. For an oscillatory instability, $\omega_i \neq 0$, and neutral stability is a stationary oscillation as shown in the fourth schematic. Neutral stability for non-oscillatory instability means both ω_r and ω_i are zero, as shown in the last schematic of figure 7-1. This is the case of exchange of stabilities considered here. Hence ω may be set to zero with no loss of generality.

The equations for the fluid, (6.15), and (6.16), become

$$(D^2 - k^2)^2 \tilde{u}_1 = (1 + \delta\zeta_r) v_1. \tag{7.1}$$

$$(D^2 - k^2) v_1 = -\mathrm{T} k^2 \tilde{u}_1. \tag{7.2}$$

The equations for the elastic layer, (6.21) - (6.23), become

$$\left(D^2 - \frac{k^2 l_e^2}{\chi}\right) u_{R_1} = k l_e \left(\frac{1}{\chi} - 1\right) D u_{Z_1}. \tag{7.3}$$

$$\left(D^2 - k^2 l_e^2\right) u_{\Theta_1} = 0. \tag{7.4}$$

$$\left(D^2 - \chi k^2 l_e^2\right) u_{Z_1} = k l_e (\chi - 1) D u_{R_1}. \tag{7.5}$$

The kinematic boundary conditions at the fluid-elastic interface are now

$$\tilde{u}_1 = 0. \tag{7.6}$$

$$v_1 = R_1 (1 - \xi) u_{R_1}. \tag{7.7}$$

$$D\tilde{u}_1 = 0. \tag{7.8}$$

and the dynamic boundary conditions at this interface are

$$-2D^3 \tilde{u}_1 = \frac{1}{l_e}(2\mu + \lambda) D u_{R_1} + k\lambda u_{Z_1}. \tag{7.9}$$

$$D v_1 = \frac{\mu \mathrm{Re}}{l_e} D u_{\Theta_1}. \tag{7.10}$$

$$2D^2\tilde{u}_1 = \mu(1 + 2D\overline{u}_R)\,u_{R_1} - \frac{\mu}{kl_e}Du_{Z_1}. \tag{7.11}$$

The kinematic boundary condition (7.7) reduces to the rigid wall boundary condition of the traditional Taylor-Couette flow for the speed $\xi = 1$. This is due to the rescaling in chapter 6. and not a physical phenomenon.

Equations (7.1). and (7.2) are solved by an expansion method similar to the one used in Yih (1987). and in McHugh (1997). The expansion contains parameters α_n. which depend on the interfacial conditions. and hence on the elastic layer. The perturbation velocity v_1 is expanded in a Fourier-series.

$$v_1 = \sum_{n=1}^{\infty} b_n \sin(\alpha_n \zeta_r). \tag{7.12}$$

The parameters α_n are determined by the kinematic boundary condition (7.7). The perturbation displacements.

$$\begin{aligned} u_{R_1} &= C_1 \sinh(kl_e\zeta_R) + C_2\zeta_R \sinh(kl_e\zeta_R) + \\ &\quad + C_3 \cosh(kl_e\zeta_R) + C_4\zeta_R \cosh(kl_e\zeta_R), \end{aligned} \tag{7.13}$$

$$\begin{aligned} u_{Z_1} &= -\left(\frac{1}{kl_e}\frac{\lambda+1}{\lambda-1}C_2 + C_3\right)\sinh(kl_e\zeta_R) - C_4\zeta_R \sinh(kl_e\zeta_R) - \\ &\quad - \left(\frac{1}{kl_e}\frac{\lambda+1}{\lambda-1}C_4 + C_1\right)\cosh(kl_e\zeta_R) - C_2\zeta_R \cosh(kl_e\zeta_R). \end{aligned} \tag{7.14}$$

are the exact solutions of equations (7.3). and (7.5). The coefficients. C_1. C_2. C_3. C_4. in equations (7.13), and (7.14). are shown in appendix C. They are determined by the dynamic boundary conditions (7.9). and (7.11). and by the no-displacement conditions (5.59). It appears. that the coefficient C_3 is equal to the displacement u_{R_1} at R_0. Hence. C_3 is

substituted for u_{R_1} in the kinematic boundary condition (7.7), which becomes

$$v_1 = R_1(1-\xi)C_3. \tag{7.15}$$

Note, the coefficient C_3 is a function of α. Substitute equations (7.12), and (C.1) into equation (7.15), rearrange, and obtain an equation with the unknowns α_n,

$$\sum_{n=1}^{\infty} b_n \sin(\alpha_n \zeta_r) - R_1(1-\xi)\sum_{n=1}^{\infty} b_n f(\alpha_n) = 0, \tag{7.16}$$

where

$$C_3 = \sum_{n=1}^{\infty} b_n f(\alpha_n), \tag{7.17}$$

and $f(\alpha_n)$ represents terms in C_3, equation (C.1), which depend on α_n. The values of α_n are the roots of equation (7.16). They are determined by the bisection method.

Substitute equation (7.12) into equation (7.1), and solve the differential equation to obtain

$$\begin{aligned} \tilde{u}_1 = \sum_{m=1}^{\infty} \frac{b_m}{(\alpha_m^2+k^2)^2} \Big[& A_1^{(m)} \cosh(k\zeta_r) + B_1^{(m)} \sinh(k\zeta_r) + \\ & + A_2^{(m)} \zeta_r \cosh(k\zeta_r) + B_2^{(m)} \zeta_r \sinh(k\zeta_r) + \\ & + \frac{4\delta\alpha_m}{\alpha_m^2+k^2} \cos(\alpha_m \zeta_r) + \\ & + (1+\delta\zeta_r)\sin(\alpha_m\zeta_r)\Big]. \end{aligned} \tag{7.18}$$

The coefficients $A_1^{(m)}, A_2^{(m)}, B_1^{(m)}, B_2^{(m)}$ are given in appendix D. Now substitute equa-

tion (7.12), and (7.18) into equation (7.2).

$$\sum_{n=1}^{\infty} b_n \left(\alpha_n^2 + k^2\right) \sin(\alpha_n \zeta_r) -$$

$$- Tk^2 \sum_{m=1}^{\infty} \frac{b_m}{(\alpha_m^2 + k^2)^2} \Big[A_1^{(m)} \cosh(k\zeta_r) + B_1^{(m)} \sinh(k\zeta_r) +$$

$$+ A_2^{(m)} \zeta_r \cosh(k\zeta_r) + B_2^{(m)} \zeta_r \sinh(k\zeta_r) + (1 + \delta\zeta_r) \sin(\alpha_m \zeta_r) +$$

$$+ \frac{4\delta\alpha_m}{\alpha_m^2 + k^2} \cos(\alpha_m \zeta_r) \Big] = 0. \qquad (7.19)$$

Multiply equation (7.19) by $\sin(\alpha_l \zeta_r)$ and integrate from 0 to 1 to obtain a set of algebraic equations in terms of the coefficients b_m. These equations may be put in matrix form.

$$[\mathbf{A} - T\mathbf{B}]\vec{b} = 0. \qquad (7.20)$$

The matrices **A** and **B** are given in appendix E.

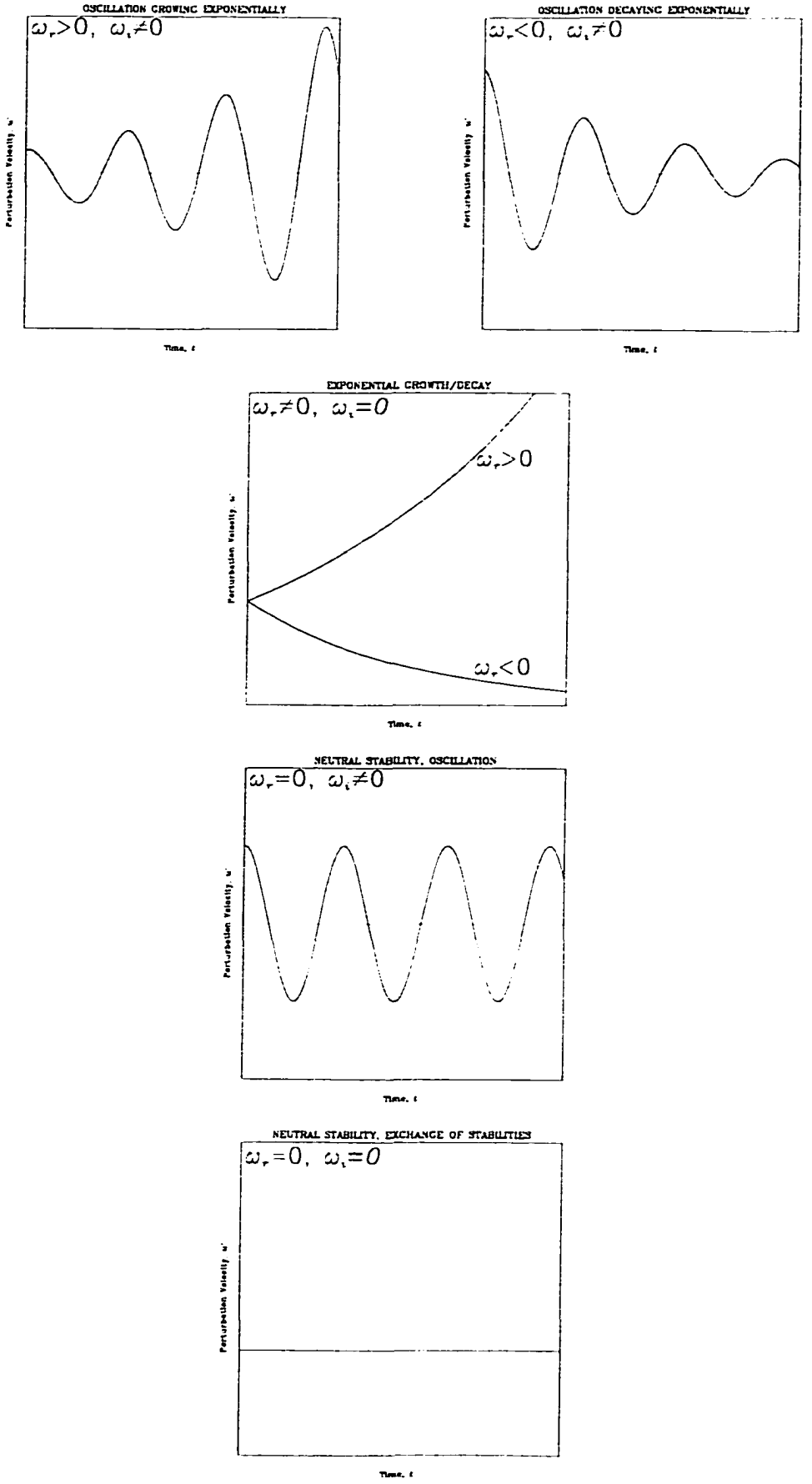

Figure 7-1: Temporal behavior of disturbance solution.

CHAPTER 8

RESULTS

The problem studied here is similar to the classical Taylor-Couette problem, which concerns flow between concentric rotating cylinders which are rigid. The present results approach the classical results asymptotically as λ and μ go to infinity, as will be seen, and the classical results are used for comparison. A few pertinent classical results are listed below:

- axisymmetric disturbances are most unstable for speeds $\xi > -0.78$:
- there is a bifurcation at the critical Taylor number from steady Couette flow to steady Taylor vortex flow, hence the exchange of stabilities is valid:
- for linear stability theory there is always a finite nonzero Taylor number for any given speed, such that the flow is stable below this critical Taylor number:

	ELASTIC LAYER	SOLID CYLINDERS
N	Taylor mode	Taylor mode
2	3410.9	3411.7
4	3397.4	3398.4
8	3396.9	3398.0
16	3396.8	3398.0
32	3396.7	3398.0
64	3396.7	3398.0

Table 8.1: Convergence test for $\xi = 0, k = 3, R_1 = 10, l_r = 10, \lambda = \mu = 3000$.

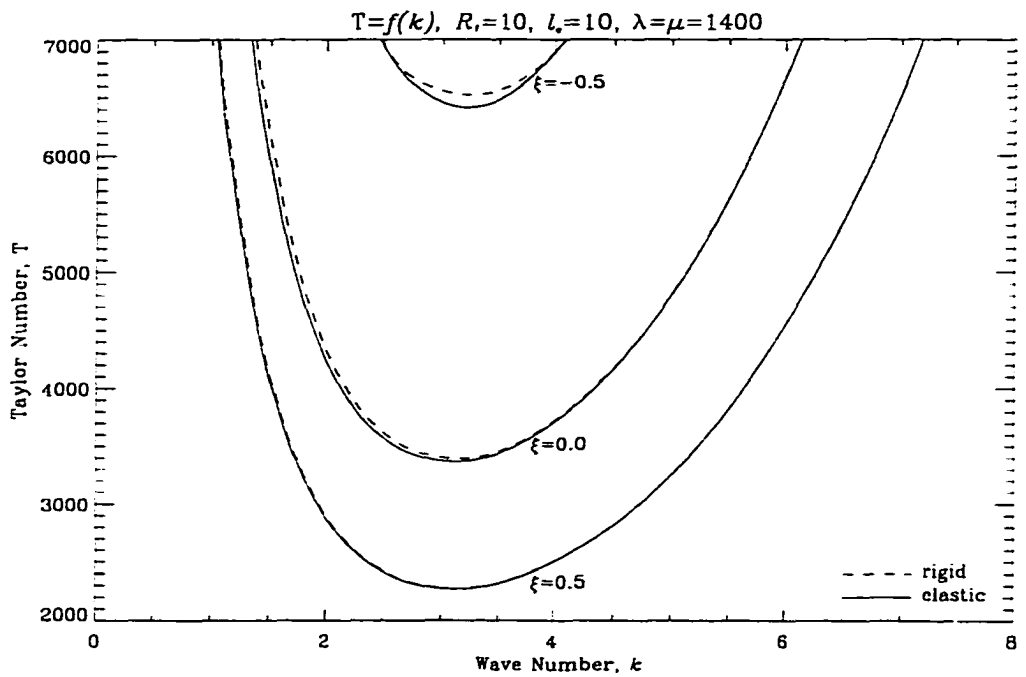

Figure 8-1: Critical Taylor number versus wave number for different speeds.

- there is an infinite set of unstable modes, called Taylor modes, for a chosen wave number and speed;

Note that the first two items have already been used to guide the assumptions of axisymmetric disturbances and neutral stability for the present work.

The present results are the critical Taylor numbers for neutral stability, which are determined by the homogeneous matrix equation given by (7.20). This matrix equation is in the form of a generalized eigenvalue problem, cf. Golub & Van Loan (1996), where the Taylor number is the eigenvalue and $\vec{b}$ is the eigenvector. The eigenvalues are calculated by converting (7.20) into a standard eigenvalue problem using the fact that A is expected to be invertible. Multiply (7.20) by the inverse of A to obtain

$$\left[\mathbf{A}^{-1}\mathbf{B} - \frac{1}{T}\mathbf{I}\right]\vec{b} = 0, \tag{8.1}$$

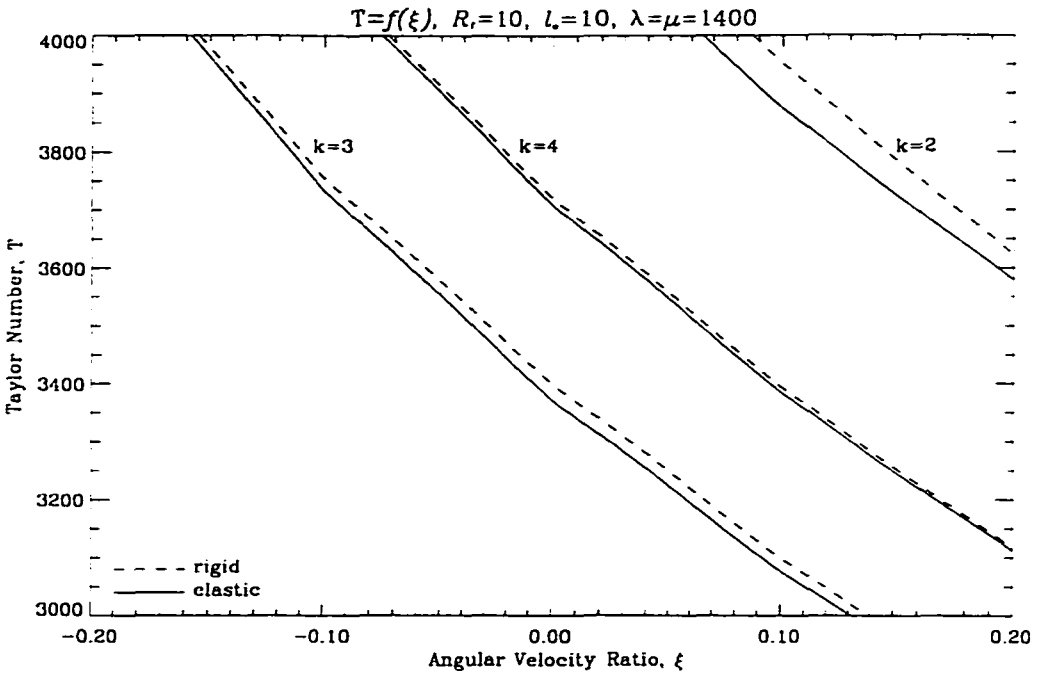

Figure 8-2: Critical Taylor number versus speed for different wave numbers.

where $\mathbf{I}$ is the identity matrix. The QR method is now used to find the eigenvalues of the matrix $\mathbf{A}^{-1}\mathbf{B}$. The inverse of the eigenvalues are the critical Taylor numbers, T. The results have been verified by treating equation (7.20) directly with a QZ method.

The first column of table 8.1 shows a convergence test of the method for an example set of parameter values. Note that the method converges rapidly: only eight expansion coefficients are needed for convergence to four significant digits, while 32 coefficients results in five significant digits. Convergence results for the classical Taylor-Couette flow with rigid walls are shown in the second column of table 8.1 using the same method, and enjoy faster convergence than the Taylor-Couette flow with an elastic layer. The rigid wall case is converged to five significant digits with only eight expansion coefficients.

The results with the elastic layer show that there is one mode which corresponds to each of the classical Taylor modes. There are no additional modes as a result of the elastic layer. Three of the critical modes are given in figure 8-1, corresponding to different speeds. The

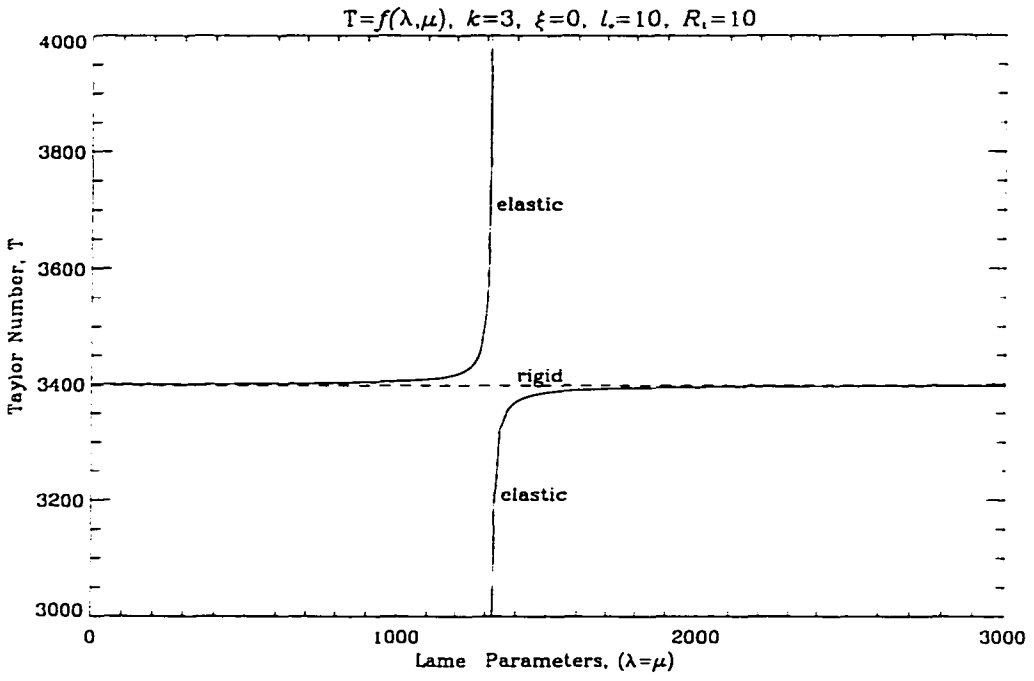

Figure 8-3: Critical Taylor number versus Lamé parameters.

critical Taylor modes for rigid walls are also shown (dashed lines). All three speeds show the same qualitative behavior. For the parameters chosen in figure 8-1, the elastic layer has a slight destabilizing effect on the traditional Taylor-Couette flow. This destabilizing effect is also seen in figure 8-2, which shows the effect of speed on the critical Taylor number, for three wave numbers.

The Lamé parameters are particularly important to the printing process, since it is possible to manipulate the stiffness of the elastic layer to control instability. The effect of the Lamé parameters is shown in figure 8-3. It can be seen in figure 8-3 that the critical Taylor number exhibits a singular behavior at one parameter value. The Taylor number approaches the rigid case as the parameters move away from this singular case: very large or very small values of λ, μ approach the rigid case. Parameter values greater than the singular value are more unstable than the rigid case, while those less than the singular value are less unstable, even becoming stable for a very narrow region of parameters. The stability issue

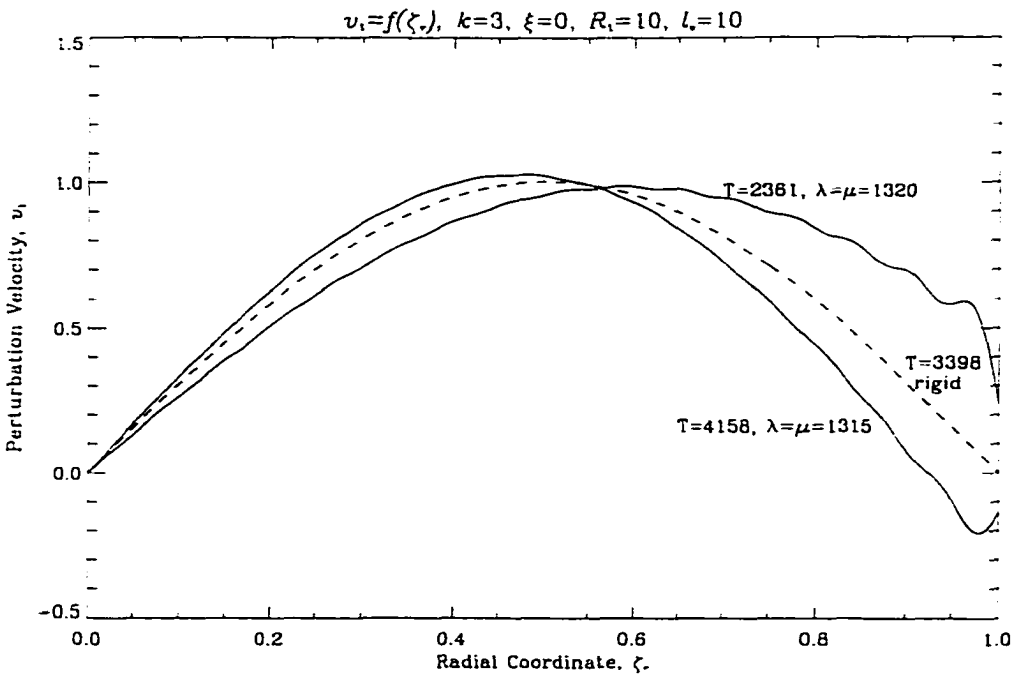

Figure 8-4: Azimuthal perturbation velocity versus rescaled radius.

at the singular point remains unclear. It seems that the solution found here is no longer valid at this point and must be reevaluated. However, the results near the singularity are converged and valid.

The singular behavior shown in figure 8-3 needs further explanation. To provide this, eigenvectors have been determined for several parameter values in the vicinity of the singular value. The eigenvectors are determined from equation (8.1) by setting the first coefficient to unity, dropping one equation, then solving the system for the remaining coefficients using LU decomposition and back/forward substitution. Figure 8-4 shows the eigenvectors for the azimuthal perturbation velocity in the fluid layer. Three eigenvectors are shown, one for rigid walls, another for Lamé parameters which are less than the singular parameter, $\lambda = \mu = 1315$, and the other for Lamé parameters greater than the singular value, $\lambda = \mu = 1320$. Figure 8-4 indicates that the smaller Taylor number gives a positive azimuthal perturbation velocity of the interface, and the higher Taylor number results in a negative

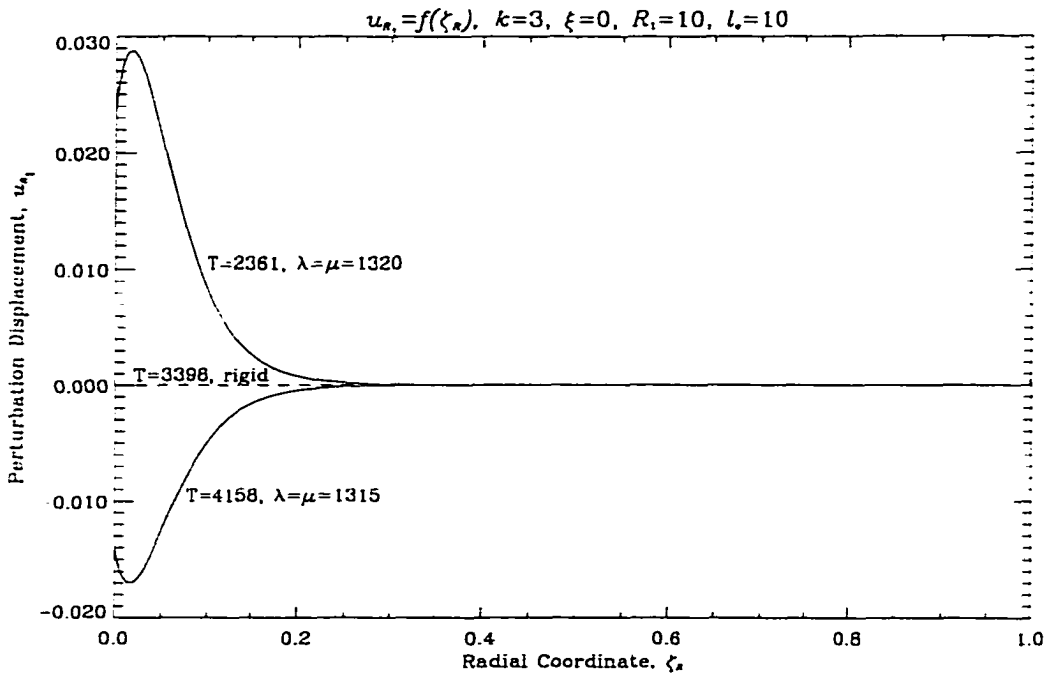

Figure 8-5: Radial perturbation displacement versus rescaled radius.

velocity of the interface. This suggests that the singular point must correspond to a sudden phase shift in the disturbance.

The azimuthal perturbation velocity in the fluid is directly coupled to the radial perturbation displacement in the solid for the neutral stability case studied here. The radial perturbation displacement in the solid is shown in figure 8-5 for the same cases of figure 8-4. Note that the same phase shift is evident in figure 8-5.

The singular behavior shown in figure 8-3 can also be obtained by varying the thickness of the elastic layer or the radius of the inner cylinder, while holding λ and μ constant, as shown in figures 8-6 and 8-7. The critical Taylor number approaches the case of rigid cylinders as either parameter changes from the singular value.

The physical reason for the singular behavior is clouded by the assumption of neutral stability. If neutral stability had not been assumed, the problem would be significantly more difficult, however it would be possible to determine a wave speed of a chosen disturbance

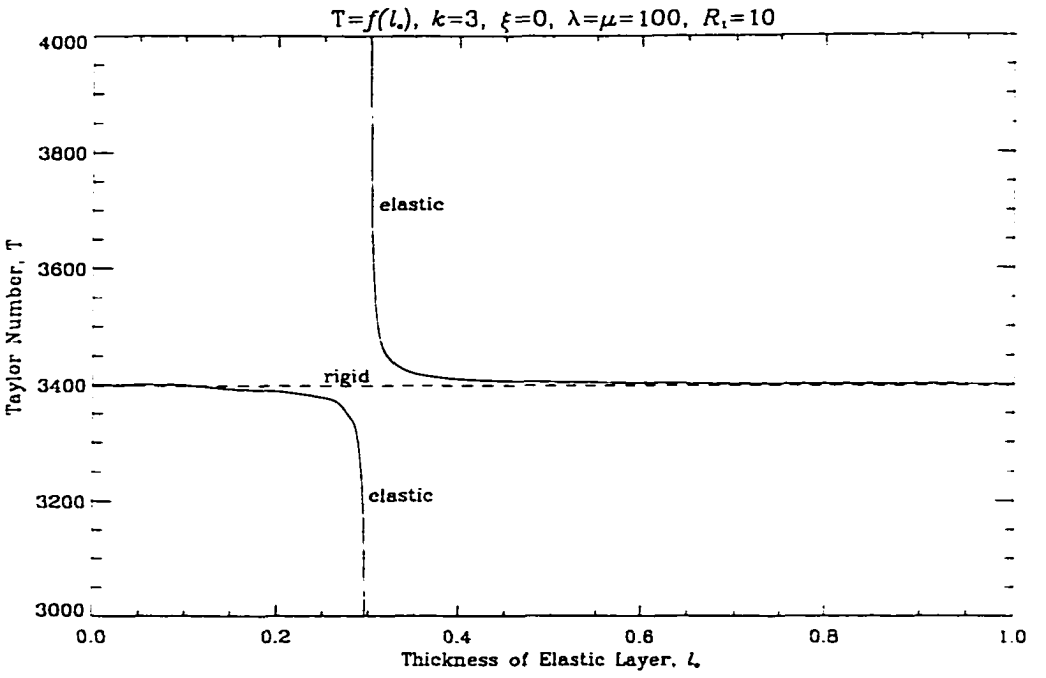

Figure 8-6: Critical Taylor number versus thickness of elastic layer.

wave. It is likely that the singular value of the parameter corresponds to the case where the wave speed is zero. This might indicate that the normal mode approach has failed at this one parameter value, and an initial value approach must be taken.

The present analysis shows that the elastic layer does not have a significant effect on the classical Taylor modes, except in the region of the afore mentioned singularity. The slight effect of the elastic layer for certain parameters agrees with the results of Denier & Hall (1991). In their study, the compliant wall was modeled by a simple equation relating the induced wall displacement to the pressure. Their results show a relatively small stabilization of longitudinal Goertler vortices over a compliant coating.

Previous work on flow over compliant coatings was briefly discussed in the introduction. It has been found by many researchers that a flexible coating will result in significantly higher critical Reynolds numbers for boundary layer modes. This phenomenon has lead to an extensive effort to achieve a drag reduction by coating ships with compliant coatings. One

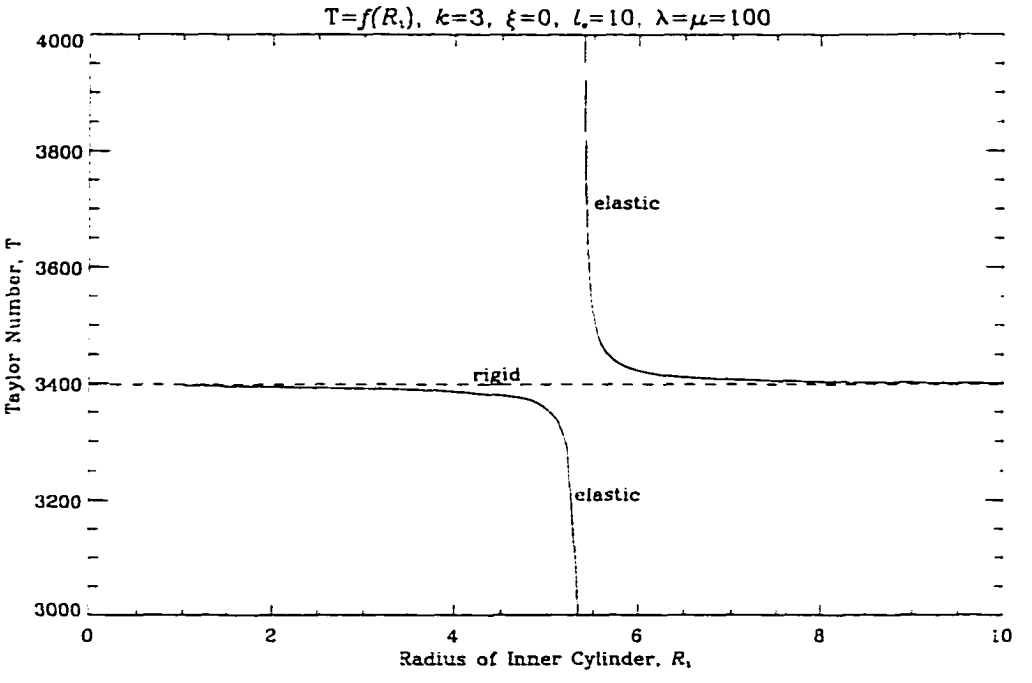

Figure 8-7: Critical Taylor number versus radius of inner cylinder.

failure of this idea was that new instabilities arise, which are associated with the interface between the fluid and the coating. These modes are generally called surface modes. The resulting waves grow on the interface and have a wavenumber vector which is parallel to the direction of the fluid flow.

The present problem does not show any surface modes. Although this is a surprise, it is most likely due to the assumption of axisymmetric disturbances. For solid cylinders, axisymmetric disturbances are known to often be the most unstable, and this lead to assuming axisymmetry here. However an axisymmetric wave does not have a component of the wavenumber vector in the azimuthal direction, which is also the direction of flow of the primary solution. Hence wavenumber vector and the primary flow cannot be parallel, and the surface modes that were expected are not present.

It is also unexpected that the effect of the elastic layer on the Taylor modes is so small. An important asymptote is reached when R_1 goes to infinity, assuming the gap and

the cylinder velocities are held fixed. This limit transforms the current problem into the cartesian problem of parallel flow over an elastic layer with a linear velocity profile, which has been studied by Benjamin (1959, 1960, 1963), Yeo (1987, 1988), and others. The effect of the elastic layer is very significant in this work. The reason that the present results do not show a significant effect may be related to the speed. Unfortunately, the present method does not converge for relatively large values of ξ, depending on the values of the other parameters. Hence the speed difference, and the strength of the shear, is limited to a relatively small value, where the centrifugal effects are more important than the shear. Larger speeds would likely show stronger effects due to the elastic layer.

The assumption of neutral stability may be the cause of this lack of convergence for higher speeds. Higher speeds mean stronger shears, which then dominate the centrifugal instability which are the Taylor modes. Shear flow instabilities generally become unstable in an oscillatory manner, which means the exchange of stability is not valid, and ω_i is not zero when $\omega_r = 0$. A treatment of larger speeds must not include the exchange of stabilities.

BIBLIOGRAPHY

ALI, H.N. & HERRON, I.H. 1996 The two-dimensional stability of a viscous fluid between rotating cylinders. *J. Math. Anal. Appl.* **203**, 481.

BENJAMIN, T.B. 1959 Shearing flow of a flexible boundary. *J. Fluid Mech.* **6**, 161.

BENJAMIN, T.B. 1960 Effects of a flexible boundary on hydrodynamic stability. *J. Fluid Mech.* **9**, 513.

BENJAMIN, T.B. 1963 Threefold classification of unstable disturbances in flexible surfaces bounding inviscid flows. *J. Fluid Mech.* **16**, 436.

BRONSTEIN, J. & SEMENDJAJEW, K. 1983 *Taschenbuch der Mathematik.* Verlag Harri Deutsch.

CARPENTER, P.W. 1990 Status of transition delay using compliant walls. Appeared in Viscous Drag Reduction in Boundary Layers, edited by D.M. Bushnell and J.N. Hefner. *Progress in Astronautics and Aeronautics.* **123**, 79.

CARPENTER, P.W. & GARRAD, A.D. 1986 Hydrodynamic stability of flow over Kramer-type compliant surfaces. Part 2. Flow-induced surface instabilities. *J. Fluid Mech.* **170**, 199.

CHANDRASEKHAR, S. 1961 *Hydrodynamic and Hydromagnetic Stability.* Dover Publications, Inc..

CHOSSAT, P. & IOOSS, G. 1994 *The Couette-Taylor Problem.* Springer-Verlag.

DAVIS, S.H. 1969 On the principle of exchange of stabilities. *Proc. Roy. Soc. London. A.* **310**, 341.

DENIER, J.P. & HALL, P. 1991 The effect of wall compliance on the Goertler vortex instability. *Phys. Fluids A* **3**, 2000.

DI PRIMA, R.C. & SWINNEY, H.L. 1985 Instabilities and transition in flow between concentric rotating cylinders. Appeared in Hydrodynamic Instabilities and the Transition to Turbulence, edited by H.L. Schwinney and J.P. Gollub. *Topics in Applied Physics* **45**, 139.

DRAZIN, P.G. & REID, W.H. 1981 *Hydrodynamic Stability.* Cambridge University Press.

DUNCAN, J.H., WAXMAN, A.M. & TULIN, M.P. 1985 The dynamics of waves at the interface between a viscoelastic coating and a fluid flow. *J. Fluid Mech.* **158**, 177.

KOSCHMIEDER, E.L. 1993 *Bénard Cells and Taylor Vortices.* Cambridge University Press.

KRUEGER, E.R., GROSS, A., DI PRIMA, R.C. 1966 On the relative importance of Taylor-vortex and non-axisymmetric modes in flow between rotating cylinders. *J. Fluid Mech.* **24**, 521.

GOLLUB, G.H. & VAN LOAN, C.F. 1996 *Matrix Computation.* The John Hopkins University Press.

LOVE, A.E.H. 1926 *A Treatise on the Mathematical Theory of Elasticity.* Dover Publications, Inc..

MACPHEE, J. 1979 An engineer's analysis of the lithographic printing process. *TAGA Proceedings (Technical Association of the Graphic Arts, Rochester).* 1.

MCHUGH, J.P. 1997 Onset of convection in horizontal cylinders. *Submitted.*

RILEY, J.J., GAD-EL-HAK, M. & METCALFE, R.W. 1988 Compliant coatings. *Annual Review of Fluid Mechanics* **20**, 393.

SCHALL, P.J. 1996 *The Stability of Flow over an Elastic Boundary.* PhD Thesis University of New Hampshire.

SCHALL, P.J. & MCHUGH, J.P. 1996 The stability of a two-layer inviscid flow between an elastic layer and a rigid boundary. *To appear in J. Appl. Mech.* .

TAYLOR, G.I. 1923 Stability of a viscous liquid contained between two rotating cylinders. *Phil. Trans. Roy. Soc., London Ser. A*, **223**, 289.

WEHAUSEN, J.V. & LAITONE, E.V. 1960 Surface Waves. *Handbuch der Physik.* **9**, 446.

YEO, K.S. & DOWLING, A.P. 1987 The stability of inviscid flow over passive compliant walls. *J. Fluid Mech.* **183**, 265.

YEO, K.S. 1988 The stability of boundary-layer flow over single- and multi-layer viscoelastic walls. *J. Fluid Mech.* **196**, 359.

YIH, C. 1972 Spectral theory of Taylor vortices. Part II. Proof of Nonoscillation. *Arch. Rat. Mech. Anal.* **47**, 288.

YIH, C. 1987 Convective instability of a spherical fluid inclusion. *Phys. Fluids A* **30**, 36.

YIH, C. 1988 *Fluid Mechanics.* West River Press.

APPENDIX A

RELATIONS BETWEEN THE EULERIAN AND LAGRANGIAN COORDINATE SYSTEMS

This section describes the relations between the Eulerian coordinates (r, θ, z), and the Lagrangian coordinates (R, Θ, Z). These relations are used in the derivation of the interfacial conditions, between the fluid and the elastic layer. The Eulerian coordinate vector $\vec{r}$ can be expressed as a vector addition,

$$\vec{r} = \vec{R} + \vec{\eta}, \tag{A.1}$$

of the Lagrangian coordinate vector $\vec{R}$, and the displacement vector $\vec{\eta}$, as shown in figure A-1. The Eulerian vector $\vec{r}$ can be represented by its radial, and axial components.

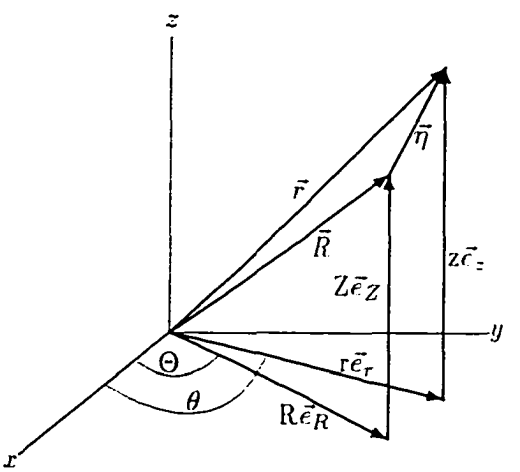

Figure A-1: Relation between Eulerian and Lagrangian coordinate systems.

$$\vec{r} = r\vec{e}_r + z\vec{e}_z. \tag{A.2}$$

Similarly, the Lagrangian vector $\vec{R}$ is

$$\vec{R} = R\vec{e}_R + Z\vec{e}_Z. \tag{A.3}$$

The displacement vector $\vec{\eta}$ can also be represented by its radial, and axial components.

$$\vec{\eta} = \alpha\vec{e}_\alpha + \gamma\vec{e}_Z. \tag{A.4}$$

where α is the radial deformation, and γ is the axial deformation, cf. figure A-2. Substitute

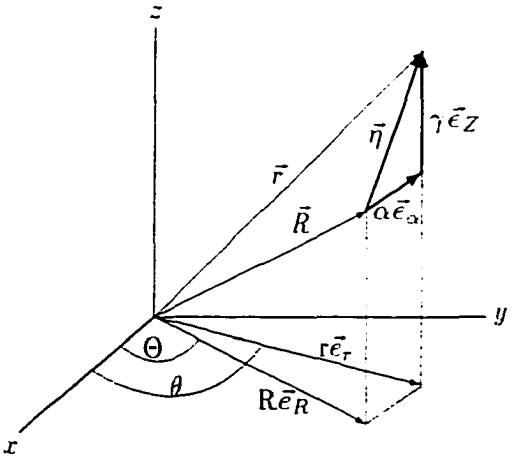

Figure A-2: Displacement vector $\vec{\eta}$ with radial component $\alpha\vec{e}_\alpha$, and axial component $\gamma\vec{e}_Z$.

equations (A.2), (A.3), and (A.4) into equation (A.1), which becomes

$$r\vec{e}_r + z\vec{e}_z = R\vec{e}_R + Z\vec{e}_Z + \alpha\vec{e}_\alpha + \gamma\vec{e}_Z. \tag{A.5}$$

Equation (A.5) is divided into radial components,

$$r\vec{e}_r = R\vec{e}_R + \alpha\vec{e}_\alpha. \tag{A.6}$$

and into axial components,

$$z\vec{e}_z = Z\vec{e}_Z + \gamma\vec{e}_Z. \tag{A.7}$$

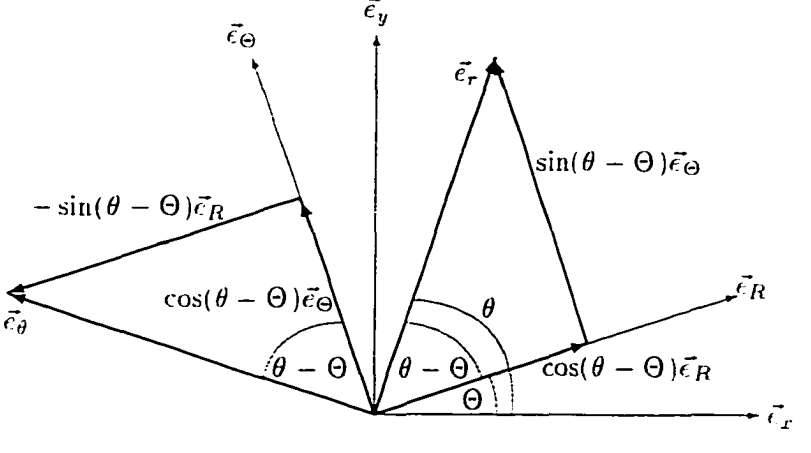

Figure A-3: Eulerian unit vector $\vec{e}_r$.

The unit vectors in the r, θ, z directions are

$$\vec{e}_r = \cos(\theta - \Theta)\vec{e}_R + \sin(\theta - \Theta)\vec{e}_\Theta. \tag{A.8}$$

$$\vec{e}_\theta = -\sin(\theta - \Theta)\vec{e}_R + \cos(\theta - \Theta)\vec{e}_\Theta. \tag{A.9}$$

$$\vec{e}_z = \vec{e}_Z, \tag{A.10}$$

respectively. Equations (A.8), and (A.9) are vector additions as seen in figure A-3. The unit vectors in axial direction are equal for the Eulerian and Lagrangian coordinate system. see equation (A.10). The Lagrangian unit vector in α direction is

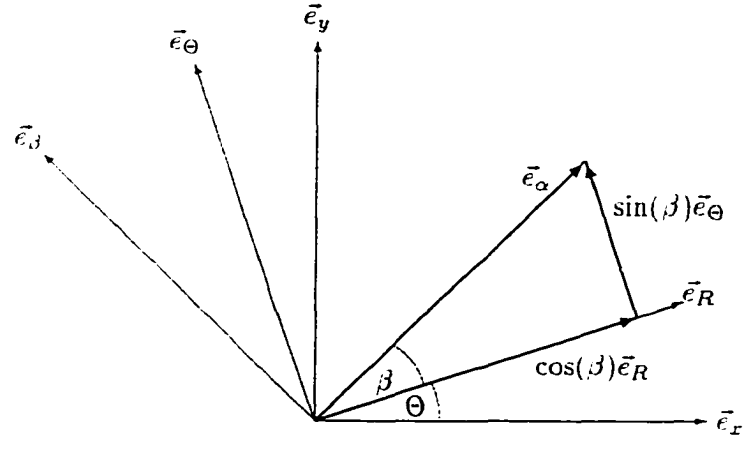

Figure A-4: Lagrangian unit vector $\vec{e}_\alpha$.

$$\vec{e}_\alpha = \cos(\beta)\vec{e}_R + \sin(\beta)\vec{e}_\Theta. \tag{A.11}$$

This is a vector addition as well. and shown in figure A-4. Substitute equations (A.8). and (A.11) into equation (A.6). equate terms of $\vec{e}_R$, and $\vec{e}_\Theta$, and solve for r and θ. which results in the Eulerian radial coordinate. and Eulerian coordinate angle.

$$r = \frac{1}{\cos(\theta - \Theta)}(R + \alpha\cos\beta). \tag{A.12}$$

$$\theta = \Theta + \arcsin\left(\frac{\alpha}{r}\sin\beta\right). \tag{A.13}$$

respectively. Substitute equation (A.10) into equation (A.7). and an equation for the Eulerian axial coordinate is obtained.

$$z = Z + \gamma. \tag{A.14}$$

The displacements in R, Θ and Z directions have the cylindrical coordinate representation in terms of α, β and γ of the following form

$$u_R = \alpha\cos\beta. \tag{A.15}$$

$$u_\Theta = \alpha\sin\beta. \tag{A.16}$$

$$u_Z = \gamma. \tag{A.17}$$

Substitute equations (A.15), (A.16), and (A.17) into equations (A.12), (A.13), and (A.14),

$$r = \frac{1}{\cos(\theta - \Theta)}(R + u_R), \tag{A.18}$$

$$\theta = \Theta + \arcsin\left(\frac{u_\Theta}{r}\right). \tag{A.19}$$

$$z = Z + u_Z. \tag{A.20}$$

respectively. The Eulerian coordinates (r, θ, z) are functions of the Lagrangian coordinates (R, Θ, Z), and displacements (u_R, u_Θ, u_Z) in R, Θ, and Z direction, respectively.

APPENDIX B

NORMAL VECTOR ON THE FLUID-ELASTIC INTERFACE

The fluid-elastic interface is expressed as an implicit mathematical function of the form

$$F(r, \theta, z; R, \Theta, Z; t) = 0. \tag{B.1}$$

cf. Wehausen & Laitone (1960). The interface changes its shape with respect to the Eulerian space (r, θ, z), the Lagrangian space (R, Θ, Z), and with respect to time t. The Lagrangian coordinates in radial, azimuthal, and axial direction are

$$R = R(r, \theta, z, t), \tag{B.2}$$

$$\Theta = \Theta(r, \theta, z, t), \tag{B.3}$$

$$Z = Z(r, \theta, z, t). \tag{B.4}$$

respectively. The Eulerian coordinates (r, θ, z) in equations (B.2) - (B.4) describe the initial position of a particle of the interface. The major deformation is expected to be in radial direction, and there exists some function $r = f(\theta, z; R, \Theta, Z; t)$, such that

$$F(r, \theta, z, t) = r - f(\theta, z; R, \Theta, Z; t) = 0. \tag{B.5}$$

Figure B-1 illustrates a differential element, dF, of the fluid-elastic interface, and the

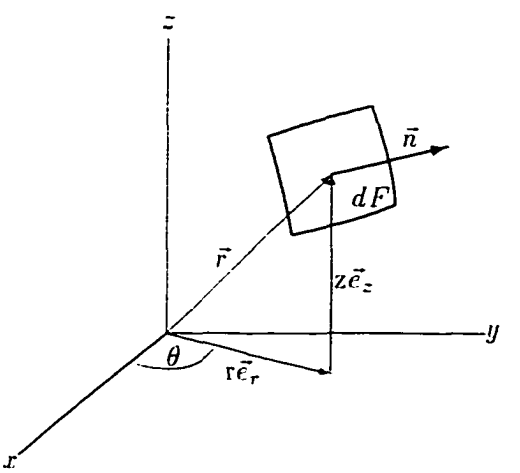

Figure B-1: Surface normal on interfacial element dF.

corresponding surface normal $\vec{n}$. The surface normal for any surface at some instant is defined in an Eulerian reference frame as

$$\vec{n} = \frac{\nabla F}{|\nabla F|}. \tag{B.6}$$

where the gradient of the surface is

$$\nabla F = \frac{\partial F}{\partial r}\vec{e}_r + \frac{1}{r}\frac{\partial F}{\partial \theta}\vec{e}_\theta + \frac{\partial F}{\partial z}\vec{e}_z. \tag{B.7}$$

and the magnitude of the gradient is

$$|\nabla F| = \sqrt{\left(\frac{\partial F}{\partial r}\right)^2 + \frac{1}{r^2}\left(\frac{\partial F}{\partial \theta}\right)^2 + \left(\frac{\partial F}{\partial z}\right)^2}. \tag{B.8}$$

Substitute equation (B.5) into equation (B.7).

$$\nabla F = 1\vec{e}_r - \frac{1}{r}\frac{\partial f}{\partial \theta}\vec{e}_\theta - \frac{\partial f}{\partial z}\vec{e}_z. \tag{B.9}$$

and substitute equation (B.5) into equation (B.8).

$$|\nabla F| = \sqrt{1 + \frac{1}{r^2}\left(\frac{\partial f}{\partial \theta}\right)^2 + \left(\frac{\partial f}{\partial z}\right)^2}. \tag{B.10}$$

Substitute equations (B.9), and (B.10) into equation (B.6), and the surface normal becomes

$$\vec{n} = \frac{1\vec{e}_r - \frac{1}{r}\frac{\partial f}{\partial \theta}\vec{e}_\theta - \frac{\partial f}{\partial z}\vec{e}_z}{\sqrt{1 + \frac{1}{r^2}\left(\frac{\partial f}{\partial \theta}\right)^2 + \left(\frac{\partial f}{\partial z}\right)^2}}. \tag{B.11}$$

The components of the surface normal are

$$\vec{n}_r = \frac{1}{|\nabla F|}\vec{e}_r. \tag{B.12}$$

$$\vec{n}_\theta = -\frac{\frac{1}{r}\frac{\partial f}{\partial \theta}}{|\nabla F|}\vec{e}_\theta. \tag{B.13}$$

$$\vec{n}_z = -\frac{\frac{\partial f}{\partial z}}{|\nabla F|}\vec{e}_z. \tag{B.14}$$

The Lagrangian radius at the interface is equal to R_0, which is the initial position of the interface, and taken to be a constant value. Equation (A.12) becomes

$$r = \frac{1}{\cos(\theta - \Theta)}(R_0 + \alpha \cos \beta). \tag{B.15}$$

Recall the definition of the function f in equation (B.5), and apply the chain rule at R_0, the derivative $\frac{\partial f}{\partial \theta}$ is

$$\frac{\partial f}{\partial \theta} = \frac{\partial r}{\partial \theta} = \frac{\partial r}{\partial \Theta}\frac{\partial \Theta}{\partial \theta} + \frac{\partial r}{\partial Z}\frac{\partial Z}{\partial \theta}. \tag{B.16}$$

similarly, the derivative $\frac{\partial f}{\partial z}$ is

$$\frac{\partial f}{\partial z} = \frac{\partial r}{\partial z} = \frac{\partial r}{\partial \Theta}\frac{\partial \Theta}{\partial z} + \frac{\partial r}{\partial Z}\frac{\partial Z}{\partial z}. \tag{B.17}$$

Take the derivative of equation (B.15) with respect to the Lagrangian coordinates Θ, and Z.

$$\frac{\partial r}{\partial \Theta} = \frac{1}{\cos(\theta - \Theta)}\left(\frac{\partial \alpha \cos\beta}{\partial \Theta} - (R_0 + \alpha\cos\beta)\tan(\theta - \Theta)\right), \tag{B.18}$$

$$\frac{\partial r}{\partial Z} = \frac{1}{\cos(\theta - \Theta)}\frac{\partial \alpha \cos\beta}{\partial Z}. \tag{B.19}$$

respectively. Note, the radial, angular, and axial deformations of the interface are

$$\alpha = \alpha(R_0, \Theta, Z), \tag{B.20}$$

$$\beta = \beta(R_0, \Theta, Z), \tag{B.21}$$

$$\gamma = \gamma(R_0, \Theta, Z), \tag{B.22}$$

respectively, cf. Appendix A. Introduce implicit mathematical functions of the form

$$G(r, \theta, z; R_0, \Theta, Z) = 0, \tag{B.23}$$

$$H(r, \theta, z; R_0, \Theta, Z) = 0, \tag{B.24}$$

and write equations (A.13), and (A.14) as

$$G = \theta - \Theta - \arcsin\left(\frac{\alpha}{r}\sin\beta\right) = 0. \tag{B.25}$$

$$H = z - Z - \gamma = 0, \tag{B.26}$$

respectively. Functions G, and H, equations (B.25), and (B.26), respectively, are functionally dependent on the implicit function of the interface, which is

$$F = r - \frac{1}{\cos(\theta - \Theta)}(R_0 + \alpha\cos\beta) = 0. \tag{B.27}$$

This is verified by obtaining zero Jacobians of the functions F, (B.27), and G, (B.25).

$$J(R, \Theta) = \frac{\partial(F, G)}{\partial(R, \Theta)} = 0. \tag{B.28}$$

and the functions F, (B.27), and H, (B.26),

$$J(R, Z) = \frac{\partial(F, H)}{\partial(R, Z)} = 0. \tag{B.29}$$

cf. Bronstein & Semendjajew (1983). The Jacobian of the functions G, H, equations (B.25), and (B.26), respectively, is

$$J(\Theta, Z) = \frac{\partial(G, H)}{\partial(\Theta, Z)}. \tag{B.30}$$

Determine the Jacobian $J(\Theta, Z)$, equation (B.30), take the derivative of equations (B.25), and (B.26) with respect to Θ, and Z, and substitute into equation (B.30). The Jacobian $J(\Theta, Z)$ in terms of α, β and γ is

$$J(\Theta, Z) = 1 + \frac{\partial \gamma}{\partial Z} + \frac{1}{r\sqrt{1 - (\frac{\alpha}{r}\sin\beta)^2}}\left(\frac{\partial(\alpha\sin\beta)}{\partial\Theta} + \frac{\partial(\alpha\sin\beta)}{\partial\Theta}\frac{\partial\gamma}{\partial Z} - \frac{\partial(\alpha\sin\beta)}{\partial Z}\frac{\partial\gamma}{\partial\Theta}\right). \tag{B.31}$$

Equation (B.31) is not equal to zero, and hence the functions G, and H are independent of each other. Substitute the relations (A.15), (A.16), and (A.17) into equation (B.31), the Jacobian $J(\Theta, Z)$ in terms of u_R, u_Θ and u_Z is

$$J(\Theta, Z) = 1 + \frac{\partial u_Z}{\partial Z} + \frac{1}{r\sqrt{1 - (\frac{u_\Theta}{r})^2}}\left(\frac{\partial u_\Theta}{\partial\Theta} + \frac{\partial u_\Theta}{\partial\Theta}\frac{\partial u_Z}{\partial Z} - \frac{\partial u_\Theta}{\partial Z}\frac{\partial u_Z}{\partial\Theta}\right). \tag{B.32}$$

The derivatives $\frac{\partial\Theta}{\partial\theta}$, and $\frac{\partial Z}{\partial\theta}$ in equation (B.16) are determined by

$$\frac{\partial\Theta}{\partial\theta} = -\frac{J(\theta, Z)}{J(\Theta, Z)} = -\frac{1}{J(\Theta, Z)}\frac{\partial(G, H)}{\partial(\theta, Z)} = \frac{1}{J(\Theta, Z)}\left(1 + \frac{\partial\gamma}{\partial Z}\right). \tag{B.33}$$

$$\frac{\partial Z}{\partial\theta} = -\frac{J(\Theta, \theta)}{J(\Theta, Z)} = -\frac{1}{J(\Theta, Z)}\frac{\partial(G, H)}{\partial(\Theta, \theta)} = -\frac{1}{J(\Theta, Z)}\frac{\partial\gamma}{\partial\Theta}. \tag{B.34}$$

respectively. Similarly, the derivatives $\frac{\partial\Theta}{\partial z}$, and $\frac{\partial Z}{\partial z}$ in equation (B.17) are determined by

$$\frac{\partial\Theta}{\partial z} = -\frac{J(z, Z)}{J(\Theta, Z)} = -\frac{1}{J(\Theta, Z)}\frac{\partial(G, H)}{\partial(z, Z)} = -\frac{1}{J(\Theta, Z)}\frac{\frac{\partial(\alpha\sin\beta)}{\partial Z}}{r\sqrt{1 - (\frac{\alpha}{r}\sin\beta)^2}}. \tag{B.35}$$

$$\frac{\partial Z}{\partial z} = -\frac{J(\Theta, z)}{J(\Theta, Z)} = -\frac{1}{J(\Theta, Z)}\frac{\partial(G, H)}{\partial(\Theta, z)} = \frac{1}{J(\Theta, Z)}\left(1 + \frac{\frac{\partial(\alpha\sin\beta)}{\partial\Theta}}{r\sqrt{1 - (\frac{\alpha}{r}\sin\beta)^2}}\right). \tag{B.36}$$

respectively. Substitute equations (B.18), (B.19), (B.33), and (B.34) into equation (B.16), the derivative $\frac{\partial f}{\partial\theta}$ in terms of α, β, and γ is

$$\begin{aligned}\frac{\partial f}{\partial\theta} = \frac{1}{J(\Theta, Z)}\frac{1}{\cos(\theta - \Theta)}\Bigg[&-\frac{\partial\gamma}{\partial\Theta}\frac{\partial(\alpha\cos\beta)}{\partial Z} + \\ &+\left(1 + \frac{\partial\gamma}{\partial Z}\right)\left(\frac{\partial(\alpha\cos\beta)}{\partial\Theta} - (R_0 + \alpha\cos\beta)\tan(\theta - \Theta)\right)\Bigg].\end{aligned} \tag{B.37}$$

Substitute equations (B.18), (B.19), (B.35), and (B.36) into equation (B.17), the derivative $\frac{\partial f}{\partial z}$ in terms of α, β, and γ is

$$\begin{aligned}\frac{\partial f}{\partial z} = \frac{1}{J(\Theta, Z)}\frac{1}{\cos(\theta - \Theta)}\Bigg[&\frac{\partial(\alpha\cos\beta)}{\partial Z} + \frac{1}{r\sqrt{1 - (\frac{\alpha}{r}\sin\beta)^2}}\Bigg(\frac{\partial(\alpha\sin\beta)}{\partial\Theta}\frac{\partial(\alpha\cos\beta)}{\partial Z} + \\ &+\frac{\partial(\alpha\sin\beta)}{\partial Z}\left((R_0 + \alpha\cos\beta)\tan(\theta - \Theta) - \frac{\partial(\alpha\cos\beta)}{\partial\Theta}\right)\Bigg)\Bigg].\end{aligned} \tag{B.38}$$

Substitute the relations (A.15), (A.16), and (A.17) into equation (B.37), the derivative $\frac{\partial f}{\partial \theta}$ in terms of u_R, u_Θ and u_Z is

$$\frac{\partial f}{\partial \theta} = \frac{1}{J(\Theta, Z)} \frac{1}{\cos(\theta - \Theta)} \left[-\frac{\partial u_Z}{\partial \Theta} \frac{\partial u_R}{\partial Z} + \right.$$
$$\left. + \left(1 + \frac{\partial u_Z}{\partial Z}\right) \left(\frac{\partial u_R}{\partial \Theta} - (R_0 + u_R) \tan(\theta - \Theta)\right) \right]. \quad \text{(B.39)}$$

Substitute the relations (A.15), (A.16), and (A.17) into equation (B.38), the derivative $\frac{\partial f}{\partial z}$ in terms of u_R, u_Θ and u_Z is

$$\frac{\partial f}{\partial z} = \frac{1}{J(\Theta, Z)} \frac{1}{\cos(\theta - \Theta)} \left[\frac{\partial u_R}{\partial Z} + \frac{1}{r\sqrt{1 - (\frac{u_m}{r})^2}} \left(\frac{\partial u_\Theta}{\partial \Theta} \frac{\partial u_R}{\partial Z} + \right. \right.$$
$$\left. \left. + \frac{\partial u_\Theta}{\partial Z} \left((R_0 + u_R) \tan(\theta - \Theta) - \frac{\partial u_R}{\partial \Theta} \right) \right) \right]. \quad \text{(B.40)}$$

The components of the normal vector, equations (B.12) - (B.14), are

$$\vec{n}_r = \frac{1}{\sqrt{1 + \frac{1}{r^2}\left(\frac{\partial f}{\partial \theta}\right)^2 + \left(\frac{\partial f}{\partial z}\right)^2}} \vec{e}_r, \quad \text{(B.41)}$$

$$\vec{n}_\theta = -\frac{\frac{1}{r}\frac{\partial f}{\partial \theta}}{\sqrt{1 + \frac{1}{r^2}\left(\frac{\partial f}{\partial \theta}\right)^2 + \left(\frac{\partial f}{\partial z}\right)^2}} \vec{e}_\theta, \quad \text{(B.42)}$$

$$\vec{n}_z = -\frac{\frac{\partial f}{\partial z}}{\sqrt{1 + \frac{1}{r^2}\left(\frac{\partial f}{\partial \theta}\right)^2 + \left(\frac{\partial f}{\partial z}\right)^2}} \vec{e}_z, \quad \text{(B.43)}$$

where the derivatives $\frac{\partial f}{\partial \theta}$, and $\frac{\partial f}{\partial z}$ are given by equations (B.39), and (B.40).

APPENDIX C

COEFFICIENTS C_1, C_2, C_3, C_4

The coefficient C_3 in the kinematic boundary condition, equation (7.15), is

$$C_3 = \frac{2}{\mu}\left(D^2\tilde{u}_1\frac{M_1}{N} - \frac{2\mu+\lambda}{k}D^3\tilde{u}_1\frac{M_2}{N}\right). \tag{C.1}$$

where

$$M_1 = (kl_e)^2(\mu+\lambda)^2 - (3\mu+\lambda)\mu\sinh^2(kl_e). \tag{C.2}$$

$$M_2 = kl_e(\mu+\lambda) - (3\mu+\lambda)\sinh(kl_e)\cosh(kl_e). \tag{C.3}$$

$$\begin{aligned} N &= 2(1+D\overline{u}_R)\left((kl_e)^2(\mu+\lambda)^2 - (3\mu+\lambda)\mu\sinh^2(kl_e)\right) - \\ &\quad -2\mu(2\mu+\lambda) + 2(2\mu+\lambda)(3\mu+\lambda)\cosh^2(kl_e). \end{aligned} \tag{C.4}$$

$$\begin{aligned} D^2\tilde{u}_1 = \sum_{m=1}^{\infty}\frac{b_m}{(\alpha_m^2+k^2)^2}\Big[&A_1^{(m)}k^2\cosh(k) + A_2^{(m)}\left(2k\sinh(k)+k^2\cosh(k)\right)+ \\ &+B_1^{(m)}k^2\sinh(k) + B_2^{(m)}\left(2k\cosh(k)+k^2\sinh(k)\right)+ \\ &+\delta\left(2\alpha_m - \frac{4\alpha_m^3}{\alpha_m^2+k^2}\right)\cos(\alpha_m) - \\ &-\alpha_m^2(1+\delta)\sin(\alpha_m)\Big]. \end{aligned} \tag{C.5}$$

$$\begin{aligned} D^3\tilde{u}_1 = \sum_{m=1}^{\infty}\frac{b_m}{(\alpha_m^2+k^2)^2}\Big[&A_1^{(m)}k^3\sinh(k) + A_2^{(m)}\left(3k^2\cosh(k)+k^3\sinh(k)\right)+ \\ &+B_1^{(m)}k^3\cosh(k) + B_2^{(m)}\left(3k^2\sinh(k)+k^3\cosh(k)\right) - \\ &-\delta\left(3\alpha_m^2 - \frac{4\alpha_m^4}{\alpha_m^2+k^2}\right)\sin(\alpha_m) - \\ &-\alpha_m^3(1+\delta)\cos(\alpha_m)\Big]. \end{aligned} \tag{C.6}$$

The coefficients $A_1^{(m)}, A_2^{(m)}, B_1^{(m)}, B_2^{(m)}$ are given in appendix D. The derivatives $D\overline{u}_R$, equation (5.49), $D^2\tilde{u}_1$, and $D^3\tilde{u}_1$ are evaluated at the fluid-elastic interface.

The coefficients C_1, C_2, C_4 are

$$C_2 = l_e k\frac{\mu+\lambda}{2\mu+\lambda}\left(\frac{1}{\mu}D^2\tilde{u}_1 - C_3(1+D\overline{u}_R)\right), \tag{C.7}$$

$$C_4 = \frac{l_e k(\mu+\lambda)(C_2 M_3 + M_4)}{(1+D\overline{u}_R)(kl_e(\mu+\lambda)\cosh(kl_e) - \mu\sinh(kl_e))}. \tag{C.8}$$

$$C_1 = -\frac{1}{k\mu}D^3\tilde{u}_1 - \frac{C_4}{kl_e(\mu+\lambda)}. \tag{C.9}$$

where

$$M_3 = \frac{(2\mu+\lambda)\cosh(kl_e)}{(\mu+\lambda)kl_e} - (1+D\overline{u}_R)\sinh(kl_e), \tag{C.10}$$

$$M_4 = \frac{1+D\overline{u}_R}{k\mu}\sinh(kl_e)D^3\tilde{u}_1 - \frac{1}{\mu}\cosh(kl_e)D^2\tilde{u}_1. \tag{C.11}$$

APPENDIX D

COEFFICIENTS A_1, A_2, B_1, B_2

The coefficients of the perturbation velocity $\tilde{u}_1$, equation (7.18), are

$$A_1^{(m)} = -4\delta \frac{\alpha_m}{\alpha_m^2 + k^2}. \tag{D.1}$$

$$A_2^{(m)} = A_1^{(m)} \Delta_1 \left[\frac{k}{\sinh k} + \cosh k - \alpha_m \sin \alpha_m - \Delta_2 \cos \alpha_m \right] + \\ + \Delta_1 \left[-\frac{\alpha_m}{k} \sinh k + (1+\delta)\Delta_2 \sin \alpha_m - (1+\delta)\alpha_m \cos \alpha_m - \delta \sin \alpha_m \right]. \tag{D.2}$$

$$B_1^{(m)} = -\frac{1}{k} \left(A_2^{(m)} + \alpha_m \right). \tag{D.3}$$

$$B_2^{(m)} = A_1^{(m)} \frac{1}{\sinh k} (\cos \alpha_m - \cosh k) + A_2^{(m)} \left(\frac{1}{k} - \coth k \right) + \\ + \frac{\alpha_m}{k} - (1+\delta) \frac{\sin \alpha_m}{\sinh k}. \tag{D.4}$$

where the constants are

$$\Delta_1 = \frac{k \sinh k}{\sinh^2 k - k^2}. \tag{D.5}$$

$$\Delta_2 = 1 + k \coth k. \tag{D.6}$$

APPENDIX E

MATRICES A AND B

$$\mathbf{A} = \frac{(\alpha_n^2 + k^2)^3}{k^2}[S1_{nm}], \tag{E.1}$$

$$\mathbf{B} = \frac{1}{\alpha_n^2 + k^2}\Big([S2_{nm}] + [S3_{nm}] + [S4_{nm}] + + [S5_{nm}]\Big) + [S6_{nm}] + [S7_{nm}]. \tag{E.2}$$

Where the entries of the matrices $[S1_{nm}], ..., [S7_{nm}]$ are of the following forms

$$S1_{nm} = \begin{cases} \frac{1}{2} - \frac{1}{4\alpha_n}\sin(\alpha_n) & \text{if } n = m. \\ \frac{1}{2}\left(\frac{\sin(\alpha_m-\alpha_n)}{\alpha_m-\alpha_n} - \frac{\sin(\alpha_m+\alpha_n)}{\alpha_m+\alpha_n}\right) & \text{otherwise.} \end{cases} \tag{E.3}$$

$$S2_{nm} = A_1^{(m)}\Big(k\sinh(k)\sin(\alpha_n) - \alpha_n\cosh(k)\cos(\alpha_n) + \alpha_n\Big). \tag{E.4}$$

$$S3_{nm} = B_1^{(m)}\Big(k\cosh(k)\sin(\alpha_n) - \alpha_n\sinh(k)\cos(\alpha_n)\Big). \tag{E.5}$$

$$S4_{nm} = A_2^{(m)}\Big(k\sinh(k)\sin(\alpha_n) - \alpha_n\cosh(k)\cos(\alpha_n) - \\ - \frac{1}{k^2+\alpha_n^2}\Big((k^2-\alpha_n^2)\cosh(k)\sin(\alpha_n) - 2k\alpha_n\sinh(k)\cos(\alpha_n)\Big)\Big). \tag{E.6}$$

$$S5_{nm} = B_2^{(m)}\Big(k\cosh(k)\sin(\alpha_n) - \alpha_n\sinh(k)\cos(\alpha_n) - \\ - \frac{1}{k^2+\alpha_n^2}\Big((k^2-\alpha_n^2)\sinh(k)\sin(\alpha_n) - 2k\alpha_n\cosh(k)\cos(\alpha_n) + 2k\alpha_n\Big)\Big). \tag{E.7}$$

$$S6_{nm} = \begin{cases} \frac{1}{2} - \frac{1}{4\alpha_n}\sin(2\alpha_n) + \delta\left(\frac{1}{4} - \frac{\sin(2\alpha_n)}{4\alpha_n} - \frac{\cos(2\alpha_n)}{8\alpha_n^2} + \frac{1}{8\alpha_n^2}\right) & \text{if } n = m. \\ \frac{1}{2}\left(\frac{\sin(\alpha_m-\alpha_n)}{\alpha_m-\alpha_n} - \frac{\sin(\alpha_m+\alpha_n)}{\alpha_m+\alpha_n}\right) + & \\ +\frac{\delta}{2}\left(\frac{\sin(\alpha_m-\alpha_n)}{\alpha_m-\alpha_n} - \frac{\sin(\alpha_m+\alpha_n)}{\alpha_m+\alpha_n} + \frac{\cos(\alpha_m-\alpha_n)-1}{(\alpha_m-\alpha_n)^2} - \frac{\cos(\alpha_m+\alpha_n)-1}{(\alpha_m+\alpha_n)^2}\right) & \text{otherwise.} \end{cases} \tag{E.8}$$

$$S7_{nm} = \frac{2\delta}{\alpha_m^2+k^2}\begin{cases} \sin^2(\alpha_m) & \text{if } n = m. \\ \alpha_m\left(\frac{\cos(\alpha_m-\alpha_n)-1}{(\alpha_m-\alpha_n)} - \frac{\cos(\alpha_m+\alpha_n)-1}{(\alpha_m+\alpha_n)}\right) & \text{otherwise.} \end{cases} \tag{E.9}$$

IMAGE EVALUATION TEST TARGET (QA-3)

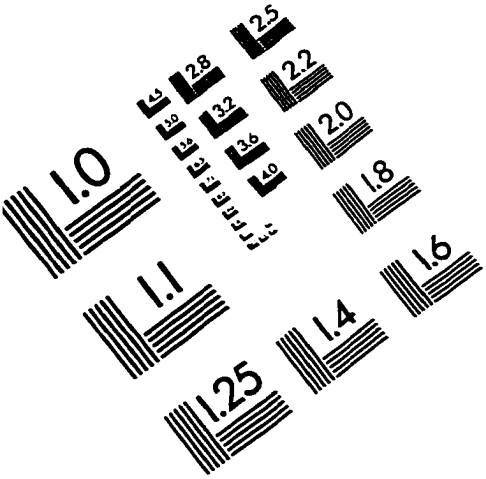

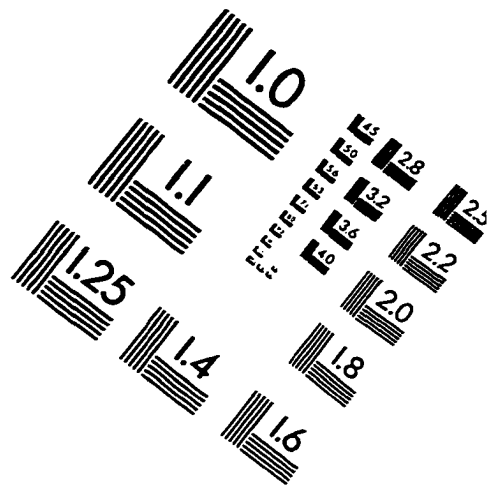

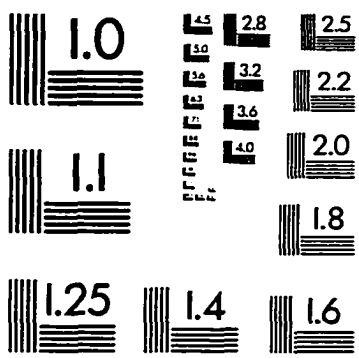

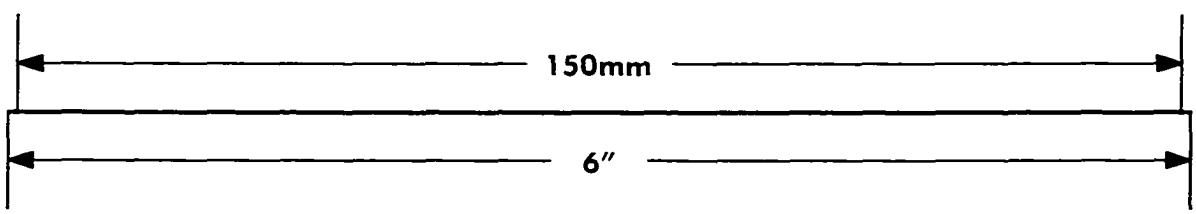

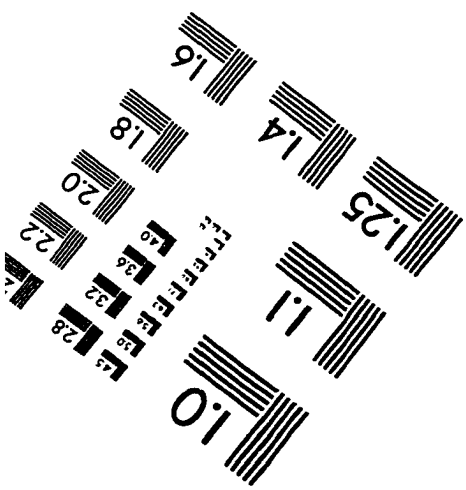

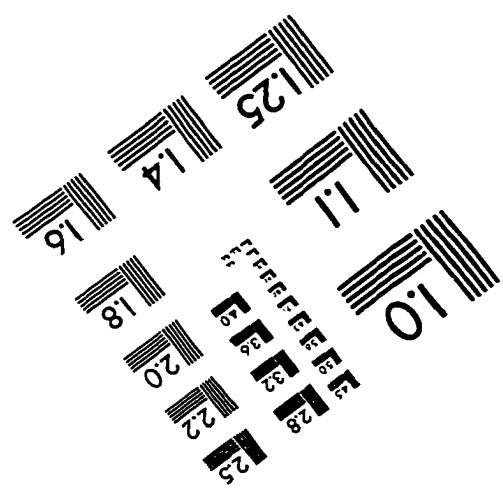

APPLIED IMAGE, Inc
1653 East Main Street
Rochester, NY 14609 USA
Phone: 716/482-0300
Fax: 716/288-5989